DNM1, a Dynamin-related Gene, Participates in Endosomal Trafficking in Yeast

Alison E. Gammie,* Laurie Jo Kurihara,* Richard B. Vallee,‡ and Mark D. Rose*

*Department of Molecular Biology, Princeton University, Princeton, New Jersey 08544-1014; and ‡Worcester Foundation for Experimental Biology, Shrewsbury, Massachusetts 01545

Abstract. We identified *DNM1*, a novel dynamin-related gene in *Saccharomyces cerevisiae*. Molecular and genetic mapping showed that *DNM1* is the most proximal gene to the right of centromere 12, and is predicted to encode a protein of 85 kD, designated Dnm1p. The protein exhibits 41% overall identity with full-length dynamin I and 55% identity with the most highly conserved 400–amino acid GTPase region. Our findings show that like mammalian dynamin, Dnm1p participates in endocytosis; however, it is unlikely to be a cognate homologue. Cells with a disruption in the *DNM1* gene showed mating response defects consistent with a delay in receptor-mediated endocytosis. The half-life of the Ste3p pheromone receptor was increased two- to threefold in the *dnm1* mutant, demonstrating that Dnm1p participates in the constitutive turnover of the receptor. To define the step in the endocytic pathway at which Dnm1p acts, we analyzed mutant strains at both early and late steps of the process. Initial internalization of epitope-tagged pheromone receptor or of labeled pheromone proceeded with wild-type kinetics. However, delivery of the internalized receptor to the vacuole was greatly impeded during ligand-induced endocytosis. These data suggest that during receptor-mediated endocytosis, Dnm1p acts after internalization, but before fusion with the vacuole. The *dnm1* mutant was not defective for sorting of vacuolar proteins, indicating that Dnm1p is not required for transport from the late endosome to the vacuole. Therefore, we suggest that Dnm1p participates at a novel step before fusion with the late endosome.

THE dynamin-related proteins are a ubiquitous superfamily of high molecular weight GTPases (reviewed in Vallee and Okamoto, 1995). The homologous region among the superfamily members is usually confined to the first 300–400 amino acids and includes the tripartite GTP binding consensus site. The superfamily can be classified into four subgroups based on homology and function.

One of the largest subgroups is composed of proteins that are closely related to mouse Mx1 (Staeheli et al., 1986). Mx proteins have been identified in at least eight different mammals (Genbank data base) and appear to function in a similar fashion in viral resistance (reviewed in Arnheiter and Meier, 1990). The precise cellular role of these proteins is not yet clear, although the GTPase activity is important for viral resistance (Nakayama et al., 1991).

The second major group, the dynamins, is comprised of proteins that are over 68% identical to dynamin isoforms (Obar et al., 1990; Faire et al., 1992; Nakata et al., 1993; Sontag et al., 1994; Cook et al., 1994) or to the shibire gene products of *Drosophila* (Chen et al., 1991; van der Bliek and Meyerowitz, 1991). shibire plays an important role in synaptic vesicle recycling (Poodry and Edgar, 1979; Koenig et al., 1983; Kosaka and Ikeda, 1983*a*) by functioning in the initial stages of endocytosis (Kosaka and Ikeda, 1983*b*; Kessell et al., 1989; Masur et al., 1990). Dynamin I is the major substrate for protein kinase C in nerve terminals, and is quantitatively dephosphorylated in parallel with synaptic vesicle cycling (Robinson et al., 1993; Sontag et al., 1994). In addition, dominant-negative mutations in rat brain dynamin block early steps of endocytosis of the transferrin receptor (Herskovits et al., 1993*a*; van der Bliek et al., 1993) at the point of coated vesicle formation (Damke et al., 1994; Takei et al., 1995; Hinshaw and Schmid, 1995). The pleiotropic effects of *shibire* mutations (Poodry et al., 1973; Chen et al., 1991; Chen et al., 1992) and the widespread tissue distribution of dynamin isoforms led to the hypothesis that dynamins play a more general role in endocytosis and membrane function. Although not all isoforms and organism variants have been tested for function, the dynamin subfamily appears thus far to participate in a similar cellular process, endocytosis.

Two additional dynamin-related proteins, Vps1p and Mgm1p, have been identified in *Saccharomyces cerevisiae*. Neither protein falls readily into the dynamin/shibire or

Address all correspondence to Mark D. Rose, Dept. of Molecular Biology, Princeton University, Princeton, NJ 08544-1014. Tel.: (609) 258-2804. Fax: (609) 258-6175.

Mx subgroups, although Vps1p is most like the former with respect to homology. *VPS1/SPO15* (Rothman et al., 1990; Yeh et al., 1991), is required for proper delivery of proteins destined for the yeast lysosome known as the vacuole (Rothman et al., 1990; Vater et al., 1992), and for retention of Golgi membrane proteins (Wilsbach and Payne, 1993). Vps1p is postulated to function in the formation of Golgi-derived vesicles destined for the vacuole (Nothwehr et al., 1995). Mgm1p is needed for maintenance of the mitochondrial genome (Jones and Fangman, 1992; Guan et al., 1993) and bears the least resemblance to any other superfamily member in terms of both homology and function. In this paper, we investigated the cellular role of a third *Saccharomyces cerevisiae* dynamin-related protein, Dnm1p. Although Dnm1p was most like Vps1p in terms of overall homology, the primary function appeared to be in endocytosis rather than vacuolar protein sorting.

Like animal cells, yeast undergo both receptor-mediated, and fluid-phase endocytosis. Receptor-mediated endocytosis occurs for the yeast peptide mating pheromone receptors, Ste2p and Ste3p (see review of Sprague and Thorner, 1992). Ste2p and Ste3p are seven-transmembrane segment receptors and are internalized constitutively (Jenness and Spatrick, 1986; Davis et al., 1993) and in response to their respective ligands, α-factor (Chvatchko et al., 1986; Jenness and Spatrick, 1986; Schandel and Jenness, 1994) and **a**-factor (Davis et al., 1993). The internalized receptors and pheromone traverse the cell in a vesicle-mediated fashion (Singer and Riezman, 1990; Singer-Krüger et al., 1993) to the vacuole where they are degraded (Chvatchko et al., 1986). Unlike some mammalian receptors, the Ste2p pheromone receptor is not recycled after ligand-induced endocytosis (Jenness and Spatrick, 1986). In contrast, fluid-phase endocytosis is commonly measured by the ability of yeast cells to internalize a soluble fluorescent dye, Lucifer Yellow (LY)[1] (Riezman, 1985; Dulic et al., 1991). Fluid-phase and receptor-mediated endocytosis appear to share some functional components, since mutants with defects in fluid-phase uptake also show receptor-mediated abnormalities (Munn and Riezman, 1994).

The yeast endocytic components to date may be roughly divided into two groups: those that contribute to internalization, and those that effect efficient delivery of endosomes to the vacuole. Mutations in the genes encoding End3p, End4p/Sla2p (Raths et al., 1993; Bénédetti et al., 1994), End6p/Rvs161p, End8p, End9p, End10p (Munn and Riezman, 1994), Sac6p/fimbrin, Act1p/actin (Kübler and Riezman, 1993), and clathrin heavy chain (Payne et al., 1988; Tan et al., 1993) all effect the internalization step of endocytosis.

The second class of endocytosis mutants effect delivery of internalized material to the vacuole. Certain secretory mutants show fluid phase (Riezman, 1985) and phospholipid (Kean et al., 1993) endocytic defects. In addition, other trafficking proteins that are important for proper vacuolar protein sorting appear to function in the endocytic pathway. The dual function of this class of proteins provided evidence that the endocytic and secretory pathways merge. This class includes small GTPases, or Rab-like proteins, Ypt7p (Wichmann et al., 1992; Schimmöller and Riezman, 1993), Ypt51p/Vps21p, Ypt52p, and Ypt53p (Singer-Krüger et al., 1994), that have been implicated in both endocytosis and vacuolar protein sorting. Other proteins involved in both pathways include End1p/Vps11 (Dulic and Riezman, 1989), Ren1p/Vps2p (Davis et al., 1993), End12p/Vps34p and End13p/Vps4p (Munn and Riezman, 1994). In summary, all of the previously identified endocytic proteins that participate in the delivery of endocytosed material to the vacuole have either a secretory, or a vacuolar protein sorting role as well.

We identified a novel dynamin-related gene in yeast, and characterized a strain in which the gene had been disrupted. The primary defect occurred at a late step of endocytosis: after internalization, but before delivery to the vacuole. The phenotypes of the mutant place Dnm1p at a unique position in the yeast endocytic pathway. Dnm1p represents the first protein to act at the endosomal trafficking stage of endocytosis that does not appear to participate in secretion or vacuolar protein sorting.

Materials and Methods

DNA Manipulations

Cloning and DNA hybridization methods were conducted as described elsewhere (Sambrook et al., 1989). Yeast genomic DNA was purified according to Rose et al. (1990). The *DNM1* disruption plasmid, pMR2357, was made by cloning *HIS3* into the region of *DNM1* encoding the conserved GTPase domain (Fig. 1 *A*). A 1.7 kb BamHI fragment containing *HIS3* from pB886 (provided by J. Broach, Princeton University) was ligated into the EcoRI site of pMR2310 after blunting the ends with the Klenow fragment of DNA polymerase I. pMR2310 contained a 0.9-kb BglII-MluI fragment of *DNM1*. A complete deletion of *DNM1* (Fig. 1 *A*) was made using the γ method of Sikorski and Hieter (1989). The 5-kb NaeI fragment from pMR2738, a *DNM1* deletion clone containing downstream sequences, was ligated to a 700-bp SmaI-MscI fragment containing upstream sequences (bp -300 to 400 in Fig. 1 *A*) creating plasmid pMR2969.

Strains, Media, and Genetic Methods

Yeast strains used in this study are listed in Table I. Yeast media and genetic techniques were as described by Rose et al. (1990). For carbon source utilization experiments, isogenic wild type (MS2288), single (MS2961, MS3128, and MS3165), double (MS3129, MS3163, MS3164), and triple deletion (MS3162) strains were streaked on YEP plates with different carbon sources and incubated at 13, 23, 30, and 37°C. Carbon sources tested were glucose, acetate, ethanol, glycerol, lactate, and glycerol plus ethanol. Bacterial strains (XL1-Blue and HB101) were manipulated as described in Sambrook et al. (1989). Yeast strains were transformed using lithium acetate (Ito et al., 1983).

Gene disruptions and deletions were constructed as described by Rothstein (1991). To disrupt *DNM1*, cells were transformed with a gel purified 2.7-kb ApaI to SacII fragment from pMR2357. To confirm the disruption, candidate transformants were analyzed by Southern blotting (Rose et al., 1990). To make a complete deletion of *DNM1*, MS3173, containing the *dnm1* disruption was transformed with the 4.9-kb PmlI and EcoRI fragment from pMR2969. The desired integrant replaced the *dnm1::HIS3* insertion with the deletion marked by *URA3*. The presence of the deletion in Ura^+, His^- transformants was confirmed by Southern blot hybridization. *VPS1* deletions were constructed using pCKR3A (T. Stevens, University of Oregon, Eugene, OR) cut with XbaI and SacI. Transformants were confirmed to be *vps1::LEU2* by Western blotting with rabbit polyclonal α-Vps1p (also from T. Stevens) and PCR amplification of genomic DNA. *MGM1* was deleted using a *mgm1::URA3* construct obtained from W. Fangman (University of Washington, Seattle, WA). Transformants were confirmed by their failure to grow on media with glycerol as the sole carbon source and by Southern blot hybridization. Double and triple dy-

1. *Abbreviations used in this paper*: CPY, carboxypeptidase Y; LY, lucifer yellow; PH, pleckstrin homology.

Table I. Yeast Strains Used in This Study

Strain	Genotype	Source
MS2288	*MAT***a** *leu2-3, 112 his3Δ200 trp1Δ1 ura3-52*	This Study
MS2961	*MAT***a** *leu2-3, 112 his3Δ200 trp1Δ1 ura3-52 dnm1::HIS3*	This Study
MS3031	*MATα ade2-101 leu2-3, 112 his3Δ200 ura3-52 dnm1::HIS3*	This Study
MS3107	*MATα ade2-101 leu2-3, 112 his3Δ200 ura3-52*	This Study
MS3128	*MAT***a** *leu2-3, 112 his3Δ200 trp1Δ1 ura3-52 vps1::LEU2*	This Study
MS3129	*MAT***a** *leu2-3, 112 his3Δ200 trp1Δ1 ura3-52 vps1::LEU2 dnm1::HIS3*	This Study
MS3161	*MATα ade2-101 leu2-3, 112 his3Δ200 ura3-52 vps1::LEU2*	This Study
MS3162	*MAT***a** *leu2-3, 112 his3Δ200 trp1Δ1 ura3-52 vps1::LEU2 dnm1::HIS3 mgm1::URA3*	This Study
MS3163	*MAT***a** *leu2-3, 112 his3Δ200 trp1Δ1 ura3-52 vps1::LEU2 mgm1::URA3*	This Study
MS3164	*MAT***a** *leu2-3, 112 his3Δ200 trp1Δ1 ura3-52 dnm1::HIS3 mgm1::URA3*	This Study
MS3165	*MAT***a** *leu2-3, 112 his3Δ200 trp1Δ1 ura3-52 mgm1::URA3*	This Study
MS3172	*MAT***a** *bar1::LEU2 leu2-3, 112 his3Δ200 trp1Δ1 ura3-52*	This Study
MS3173	*MAT***a** *bar1::LEU2 leu2-3, 112 his3Δ200 trp1Δ1 ura3-52 dnm1::HIS3*	This Study
MS3349	*MATα ade2-101 leu2-3, 112 his3Δ200 ura3-52 dnm1::HIS3 vps1::LEU2*	This Study
MS3385	*MATα pep4::LEU2 ade2-101, leu2-3, 112 his3Δ200 ura3-52 dnm1::HIS3*	This Study
MS3386	*MATα pep4::LEU2 ade2-101, leu2-3, 112 his3Δ200 ura3-52*	This Study
MS3666	*MAT***a** *ade2-101 ura3-52 his3Δ200 leu2-3,112*	This Study
MS3827	*MATα ste3Δade2-101 leu2-3, 112 his3Δ200 ura3-52*	This Study
MS3832	*MATα ste3Δade2-101 leu2-3, 112 his3Δ200 ura3-52 dnm1::HIS3*	This Study
MS3833	*MAT***a** *bar1::LEU2 leu2-3, 112 his3Δ200 trp1Δ1 ura3-52 dnm1Δ::URA3*	This Study
MY1992	*MAT***a** *ade2 his6 met1 ura1 can1 cyh1 rme sst1*	J. Broach, Princeton University
MY3468	*MAT***a** *cdc28-4 leu2-3, 112 his3Δ200 ura3-52*	This Study
MY3542	*MAT***a** *cdc28-4 leu2-3, 112 his3Δ200 ura3-52 dnm1::HIS3*	This Study
SY1372	*MATα ste3Δ ura3-52 met14 ade2-1 ade1 his6 trp1^{am}*	G. Sprague, University of Oregon

namin-related deletion strains were constructed by sequential disruptions and confirmed by the methods listed for each gene.

The *bar1* deletion strains were constructed using pZV77 (G. Sprague, University of Oregon). Expression of the Bar1 protease was assayed (Sprague, 1991) using MY1992 as a tester lawn (see Table 1). The *pep4* deletion strains were constructed with pTS17 (T. Stevens). Transformants were assayed for loss of *PEP4* function by the method of Jones (1977). Deletions of *STE3* were obtained by the two step gene replacement method (described in Rothstein, 1991) using pDH107 (G. Sprague). The *ste3* deletion phenotype was confirmed by the failure of the *MATα* cells to mate.

Polymerase Chain Reaction

Degenerate primers based on homology with rat brain dynamin (Obar et al., 1990), mouse Mx1 (Staeheli et al., 1986), and Vps1p (Rothman et al., 1990) were used in the following combinations, (*a*) 514 and 512, (*b*) 514 and 513, (*c*) 515 and 512, and (*d*) 515 and 513. Primer sequences and degeneracy were: 514:GGGAATTCGGXAA(G/A)(T/A)(C/G)X(T/A)(C/G)XGTX(C/T)TXGA 65,536-fold; 515:GGGAATTC(T/C)TXCCX(A/C)GXGGX(A/T)(C/G)XGGXAT, 65,536-fold; 512: GGGGATCCXCCXGGXA(G/A)(A/G)TCXAXXA(G/A)XGT, 131,072-fold; and 513: GGGGATCC(C/T)TTXGTXAGXACXCC(G/T/A)ATXGT, 6,144-fold. PCR was conducted in 50 μl under mineral oil (Sigma, St. Louis, MO). Reaction conditions were 10 mM Tris-HCl, pH 8.3, 50 mM KCl, 1.5 mM $MgCl_2$, 100 pmol of each primer, 200 μM deoxynucleotides dATP, dCTP, dGTP, and dCTP, (Pharmacia LKB Nuclear, Gaithersburg, MD), 2.5 μg genomic DNA and 1.25 U of Taq Polymerase (Perkin-Elmer Cetus, Norwalk, CT). Yeast strains were SF838-1Dα/pCKR3 (*vps1Δ*) and SF838-1Dα (*VPS1*) from T. Stevens. Reactions were conducted as follows: 5 cycles of 95°C 1 min, 37°C 2 min, 72°C 1 min, then 25 cycles of 95°C 1 min, 42°C 2 min, 72°C 1 min. Controls were run without genomic DNA and with each primer individually. Primer 515 amplified spurious sequences when acting as sole primer. Gel purified PCR products amplified from *vps1* deletion strain DNA were digested with BamHI and EcoRI, cloned into pRS306 (Sikorski and Hieter, 1989), and sequenced. PCR reactions were repeated with genomic DNA from an isogenic wild-type strain and from the single, double, and triple deletion strains, using identical reaction conditions.

Cloning, Physical Mapping, and DNA Sequencing of DNM1

Colony hybridization of a yeast genomic library (Rose et al., 1987) in HB101 using *DNM1*-specific probes were performed according to Sambrook et al. (1989). Yeast chromosomes were electrophoretically separated, blotted to membranes and hybridized with a *DNM1*-specific probe as described in Rose et al. (1990). Prime λ-clone grid filters were obtained from Linda Riles (Washington University School of Medicine, St. Louis, MO) and probed according to the protocol provided. The *DNM1* probe hybridized to clone 4355.

Both strands of a 4.0-kb region containing the *DNM1* gene and centromere 12 (*CEN12*) were sequenced using a combination of nested deletions (Ozkaynak and Putney, 1987) and subclones in Sikorski vectors (Sikorski and Hieter, 1989). Templates were sequenced using oligonucleotides (Princeton University), α-^{35}S-dATP (Amersham Corp., Arlington Heights, IL), and the Sequenase Kit (US Biochemicals, Cleveland, OH). Stretches of the second strand were sequenced using *DNM1*-specific oligonucleotides (Princeton University).

Vacuolar Protein Sorting Assays

Strains MS3031, MS3107, MS3161, and MS3349 were grown at 30°C to mid-exponential phase, washed and diluted in fresh YEPD media to equivalent concentrations. Cells were allowed to grow an additional 2 h. Proteins in the cell pellet were processed as described by Ohashi et al. (1982). Proteins in the supernatant were precipitated by adding trichloroacetic acid to 10%. Proteins samples were separated by SDS-PAGE, and analyzed by Western blotting with a 1:5,000 dilution of rabbit α-carboxypeptidase (α-CPY) (R. Schekman, University of California at Berkeley). The secondary antibody was conjugated to horseradish peroxidase (Amersham) and bands were visualized using an ECL Western detection kit (Amersham).

For the CPY pulse–chase experiments, cells were grown in synthetic complete media at 30°C until an OD_{600} of 0.5–0.7 was reached. Cultures were washed and resuspended to 2–3 OD_{600}/ml in synthetic media lacking cysteine and methionine. Cells were starved for methionine for at least 30 min at 30°C. ^{35}S-Translabel was added to 25 to 100 μCi/OD_{600} (ICN Radiochemicals, Irvine, CA). After 10 or 15 min labeling, the chase cocktail was added to a final concentration of 0.1% cysteine, 0.1% methionine, 0.1 M $(NH_4)_2SO_4$. Aliquots were taken at the indicated times, placed on ice and treated with NaN_3 (to 10 μM) and cycloheximide (to 100 mg/ml). Cell lysis, immunoprecipitations, and autoradiography were conducted as described previously (Scidmore et al., 1993). Strains used in the assay were MS2288, MS2961, MS3128, and MS3129, (Fig. 3 *B*) or MS2288 and MS2961 (Fig. 3 *C*). The levels of P1, P2, and mature CPY were quantitated using a PhosphorImager and ImageQuant Software (Molecular Dynamics, Sunnydale, CA). Cricket Graph Software (Malvern, PA) was used to plot the rates of turnover or accumulation of the forms of CPY.

For Pho8p experiments, wild-type (MS2288) and *dnm1* (MS2961) cells were pulse labeled and chased as described above. Immunoprecipitations of Pho8p were conducted with affinity-purified α-Pho8p rabbit polyclonal antibody (a generous gift from T. Stevens, University of Oregon) as described previously (Nothwehr et al., 1995). A 6.5% SDS–polyacrylamide gel was used to resolve the bands and the precursor and mature forms were quantitated as described for CPY immunoprecipitations.

Recovery From Pheromone Arrest

MS3172 and MS3173 were grown to 10^7 cells/ml at 30°C. Cultures were split and half were exposed to 0.59 μM α-factor (synthesized at Princeton University). Pheromone treated cells were grown until the culture showed no further increase in optical density. Cells were large with single or multiple shmoo projections. Untreated cultures were grown until they reached stationary phase as determined by optical density. Cells were washed several times in fresh YEPD and diluted to 10^7 cells/ml. Recovery from pheromone arrest was assessed by three methods: (*a*) Optical density was measured by a Klett-Summerson Colorimeter (Klett MFG Co., NY), (*b*) Bud formation was assessed by microscopy, and (*c*) Viable cell number was measured by plating dilutions onto YEPD agar. Recovery from stationary phase was assessed by optical density. Recovery after nonpheromone-induced G1 arrest was tested with strains containing the *cdc28-4* mutation. MY3468 and MY3542 were cultured at 37°C for 4 h at which point the cells were fully arrested (>95% unbudded). The cultures were then incubated at 23°C and analyzed for bud formation every 15 min.

Quantitative Mating After Repression of Ste3p Synthesis

*MAT*α strains, MS3827 and MS3832, containing the *ste3* deletion, were transformed with pSL552, a plasmid with *STE3* under the *GAL1* galactose inducible promoter (G. Sprague). The strains were grown at 30°C in synthetic media lacking uracil, with 2% raffinose as the sugar source (-URA raffinose), to midexponential phase. Galactose was added to 2% and the cultures were grown for an additional 4 h at 30°C after which glucose was added to 4% to repress synthesis of Ste3p. The $t = 0$ time point represents cells mating without repression. Subsequent time points represent the time in glucose media before mating. The mating partner, MS2288, was grown in YEPD media to a concentration of 1–2 × 10^7 cells/ml. Quantitative filter matings were conducted for 6 hours as described by Rose et al. (1990). Diploids were selected on plates lacking adenine and tryptophan.

Pulse–Chase Analysis to Determine the Turnover Rate of Ste3p

Isogenic *MAT*α strains MS3031, MS3107, MS3385, and MS3386 and the negative control strains SY1372 *MAT*α *ste3Δ* (G. Sprague) and MS3666 *MAT***a** were pulse labeled for 10 min as described above for CPY sorting. The first time point ($t = 0$) was taken before the chase. Chase time points were taken at 15, 30, and 60 min. At each time point 500 μl of cells were added to an equal volume of ice-cold stop solution (20 μM NaN_3, 20 μM KF). Cells were kept on ice for 15 min and centrifuged. Cell pellets were frozen in liquid nitrogen and stored at -70°C. Proteins were solubilized as described in Davis et al. (1993). Before immunoprecipitation, the labeled extracts were preincubated with PAS (Pharmacia) for 30 min on ice. The extracts were precleared by centrifugation for 30 s at ~14,000 *g* and the supernatant was added to PAS that had been preadsorbed with α-Ste3p polyclonal antibody (from G. Sprague). The remaining steps of the immunoprecipitation were conducted as described previously (Davis et al., 1993). Separate experiments confirmed that the turnover of Ste3p was dependent on the vacuolar protease Pep4p. The half-life of Ste3p was quantitated as described for CPY.

Internalization Assays

Strains and protocols for purification the of ^{35}S-α-factor were generously provided by D. Jenness (University of Massachusetts Medical Center, Worcester, MA). Purification of ^{35}S-α-factor was described previously (Schandel and Jenness, 1984). The pheromone had a specific activity of 2 Ci/mM at the time of the binding studies. The quality of the purified pheromone was assessed by thin layer chromatography (Dulic et al., 1991). A minor oxidized product was present in the binding analyses. The ^{35}S-α-factor showed specific binding to cells expressing the Ste2p receptor (MS3173), but not to those lacking the receptor (MS3107, *MAT*α or DJ213-7-3, *MAT***a** *ste2Δ*). In addition, binding was restored to DJ213-7-3 when the *STE2* gene was provided on a plasmid (pJBK008). Finally, specific binding to cells possessing Ste2p was competitively inhibited with unlabeled pure synthetic α-factor. Internalization experiments were conducted as described in detail by Dulic et al. (1991).

Lucifer yellow accumulation was assessed as described in Dulic et al. (1991) except that the washes were conducted as specified by Munn and Riezman (1994). Exponentially growing strains MS3172 and MS3173 were incubated for 0.5, 1.0, and 1.5 h in the presence of Lucifer Yellow CH (Sigma). Photographs were taken with identical exposure times and developing conditions.

Immunofluorescence of Ste3Δ365p After Pheromone Treatment

Immunofluorescence of Ste3Δ365p after pheromone treatment was as described by Davis et al. (1993) with modifications. MS3385 and MS3386, *MAT*α *pep4* strains, were transformed with pSL2006, to express c-myc tagged Ste3Δ365p, (Nick Davis, University of Michigan). Strains were grown at 30°C in -URA raffinose synthetic media to midexponential phase. Galactose was then added to 2% and the cultures were allowed to grow for an additional 4 h. For the $t = 0$ time point, a 10-ml aliquot of the culture was taken for immunofluorescence analysis (Roberts et al., 1991). To repress further receptor synthesis, glucose was added to the remaining cultures to a final concentration of 4%. The experimental cultures were treated with an equal volume of cell-free **a**-factor culture supernatants, while the control cells were treated with equivalent supernatants from cells overexpressing α-factor (SY70). The **a**-factor supernatant was from a saturated culture of SM1587, a strain overexpressing **a**-factor (S. Micheallis, Johns Hopkins University, Baltimore, MD). The cultures were placed back at 30°C and assayed at 0.5, 1.0, and 1.5 h after pheromone treatment.

Preparation of cells for immunofluorescence was as described previously (Roberts et al., 1991) except that spheroplasting was performed with Oxalyticase (Enzogenetics, Corvalis, OR) at 20 μg/ml for 1.5 h (Davis et al., 1993). 9E10 α-c-myc (Princeton Monoclonal Facility) was the primary antibody and FITC-α-mouse IgG (Sigma) was the secondary antibody. Cells were quantitated for the percentages of staining and for the percentages of cells displaying the reported phenotype. Controls included strains carrying the YCp50 vector instead of pSL2006 and experimental cells incubated with no primary antibody.

Results

Identification of a Novel Dynamin-related Gene, DNM1

PCR was used to identify a new dynamin-related family member in *Saccharomyces cerevisiae*. We designed degenerate oligonucleotides to highly conserved regions (Fig. 1 *B*) in three family members: mouse Mx1 (Staeheli et al., 1986), Vps1p (Rothman et al., 1990), and rat brain dynamin I (Obar et al., 1990). Genomic DNA from a strain with a deletion in the *VPS1* gene was used to enrich novel family members. Two of the four possible primer combinations gave specific products. Primer combination 515-513 amplified a region of *MGM1*, a dynamin-related gene found to be important in maintenance of the mitochondrial genome (Jones and Fangman, 1992; Guan et al., 1993). Primer combination 515-512 amplified a portion of *DNM1*, a new family member. A fragment of the cloned *DNM1* PCR product was used to probe a centromeric based yeast genomic library (Rose et al., 1987). Two full-length clones, and four partial clones were obtained by screenings of the library.

The *DNM1* locus was mapped using genetic and molecular techniques. Hybridization of a *DNM1* probe to a blot of yeast chromosomes separated by pulsed-field gel electrophoresis (Rose et al., 1990) localized *DNM1* to chromosome 12 (data not shown). The placement of *DNM1* on

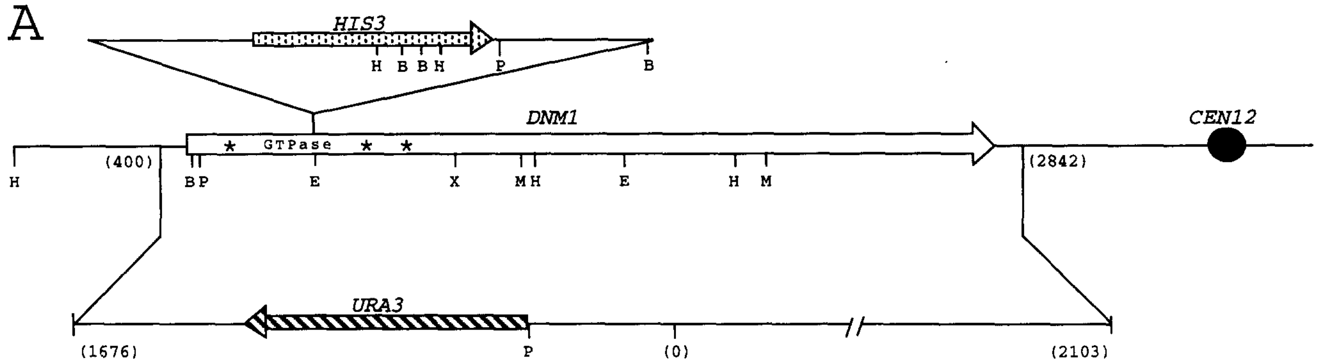

B

```
   1 AAGCTTTCACCAATATTCGTGATTTTCTATTGCTCAGAATGGCAACAAATCTTCAATCTTTAACAGGGAAGAGGGAGCATCGGGAGAGAAATCAGCCGGTTCCTCGAAGCAACATCAACA
 121 CGTTGGCGATAACAATGCTAAAACCGCGTAAAAAAGCTAAAGCCTTGCCTAAAACTTGATACATATTGATATTTATTATTTAGTACACGTATGTAGCATCGATCTTAGAAAATGCATGTT
 241 TGTATTTATTGTTAGTACCTTGATCGCCACCTTTCTAGGTAATGATAGGTCCTCAACTTTTACTACGCGGTGCACGCCTGTAAGGTCGGGCAAAACAAAGTGTGGGAACAATAAATAAGA
 361 GGGTAGGATGAAATATTACCTTTACTCTACTGCTCAGGTTGGCCACAATTTGCTAAAGAGTTTATCATTAAGTAGCTACCAGCGAATCTAAATACGACGGATAAAGAATGGCTAGTTTAG
                                                                                                                     M  A  S  L  E    5
                                                                                                              514 ────────
 481 AAGATCTTATTCCTACTGTCAACAAGCTGCAGGATGTTATGTACGACTCCGGGATCGATACACTCGATTTGCCCATTTTAGCTGTTGTTGGGTCACAATCCTCCGGGAAATCCTCGATAT
      D  L  I  P  T  V  N  K  L  Q  D  V  M  Y  D  S  G  I  D  T  L  D  L  P  I  L  A  V  V  G  S  Q  S  S  G  K  S  S  I  L   45
 ──►                   515 ──────────►                                                          *  *  *  *  *  *  *  *
 601 TGGAAACGTTAGTTGGAAGAGATTTTTTACCTAGGGGTACTGGTATTGTCACAAGAAGACCGTTAGTTCTTCAACTTAATAACATATCTCCAAATTCTCCTCTAATAGAGGAAGATGATA
      E  T  L  V  G  R  D  F  L  P  R  G  T  G  I  V  T  R  R  P  L  V  L  Q  L  N  N  I  S  P  N  S  P  L  I  E  E  D  D  N   85

 721 ACTCAGTTAATCCACATGATGAAGTTACAAAAATATCAGGATTCGAAGCTGGTACGAAGCCCTTGGAGTATAGGGGCAAGGAAAGAAATCATGCAGATGAGTGGGGGGAATTCCTGATAT
      S  V  N  P  H  D  E  V  T  K  I  S  G  F  E  A  G  T  K  P  L  E  Y  R  G  K  E  R  N  H  A  D  E  W  G  E  F  L  I  S  125

 841 CACCTGATATACCAGGAAAACGGTTTTATGATTTCGACGATATCAAAAGAGAAATCGAAAACGAAACAGCGAGGATAGCCGGTAAGGATAAGGGCATCAGTAAGATTCCGATTAATTTGA
      P  D  I  P  G  K  R  F  Y  D  F  D  D  I  K  R  E  I  E  N  E  T  A  R  I  A  G  K  D  K  G  I  S  K  I  P  I  N  L  K  165
                                ◄────────── 512
 961 AAGTGTTTTCCCCTCATGTTTTGAATCTAACGCTAGTAGATTTGCCTGGGATTACAAAGGTTCCTATTGGGGAACAACCACCTGATATTGAAAAGCAAATCAAGAATTTGATCCTAGACT
      V  F  S  P  H  V  L  N  L  T  L  V  D  L  P  G  I  T  K  V  P  I  G  E  Q  P  P  D  I  E  K  Q  I  K  N  L  I  L  D  Y  205
                                            *  *  *  *                                                            ◄──────────
1081 ATATAGCCACTCCAAATTGTTTAATCTTGGCCGTCTCTCCAGCTAACGTTGATCTTGTTAATTCTGAATCCTTAAAGTTGGCCAGAGAGGTAGACCCTCAGGGCAAAAGGACTATTGGTG
      I  A  T  P  N  C  L  I  L  A  V  S  P  A  N  V  D  L  V  N  S  E  S  L  K  L  A  R  E  V  D  P  Q  G  K  R  T  I  G  V  245
 ──────── 513
1201 TCATTACCAAATTAGATTTGATGGATTCTGGGACTAATGCTCTAGATATCTTGTCTGGAAAAATGTATCCTCTGAAATTGGGGTTTGTTGGTGTAGTGAATCGCTCGCAACAGGATATTC
      I  T  K  L  D  L  M  D  S  G  T  N  A  L  D  I  L  S  G  K  M  Y  P  L  K  L  G  F  V  G  V  V  N  R  S  Q  Q  D  I  Q  285
         *  *  *  *
1321 AATTGAACAAAACCGTTGAAGAATCATTGGACAAAGAAGAGGACTATTTCAGGAAACATCCAGTCTACAGAACTATTTCAACAAAGTGTGGTACGCGTTATTTAGCTAAATTGCTAAACC
      L  N  K  T  V  E  E  S  L  D  K  E  E  D  Y  F  R  K  H  P  V  Y  R  T  I  S  T  K  C  G  T  R  Y  L  A  K  L  L  N  Q  325

1441 AGACATTATTAAGCCACATTAGAGACAAGCTTCCGGATATTAAAACCAAGTTAAATACCCTGATCTCTCAAACCGAACAAGAGCTCGCTAGATACGGTGGCGTAGGAGCTACTACTAATG
      T  L  L  S  H  I  R  D  K  L  P  D  I  K  T  K  L  N  T  L  I  S  Q  T  E  Q  E  L  A  R  Y  G  G  V  G  A  T  T  N  E  365

1561 AAAGCAGAGCTAGCCTTGTTCTTCAACTAATGAATAAGTTTTCTACAAACTTCATTTCATCTATAGATGGTACATCCTCCGACATTAATACGAAGGAACTCTGTGGTGGTGCCCGTATTT
      S  R  A  S  L  V  L  Q  L  M  N  K  F  S  T  N  F  I  S  S  I  D  G  T  S  S  D  I  N  T  K  E  L [C  G  G  A  R  I] Y  405

1681 ATTACATTTACAATAATGTTTTTGGGAATTCTTTGAAGTCGATTGATCCAACTTCTAATTTATCCGTTCTTGATGTTAGAACAGCGATTAGAAATTCTACTGGTCCCCGTCCTACATTAT
      Y  I  Y  N  N  V  F  G  N  S  L  K  S  I  D  P  T  S  N  L  S  V  L  D  V  R  T  A  I  R  N  S  T  G  P  R  P  T  L  F  445

1801 TTGTACCTGAGTTGGCTTTTGACCTATTGGTTAAACCTCAAATTAAACTTTTACTAGAACCATCTCAACGTTGCGTCGAGTTAGTTTACGAGGAGCTGATGAAAATATGCCATAAATGTG
      V  P  E  L  A  F  D  L  L  V  K  P  Q  I  K  L  L  L  E  P  S  Q  R  C  V  E  L  V  Y  E  E  L  M  K  I  C  H  K  C  G  485

1921 GCTCCGCTGAGCTAGCTAGATATCCTAAATTGAAGAGTATGTTAATAGAAGTTATAAGCGAACTACTTAGAGAAAGGTTACAACCTACTCGCTCTTACGTTGAAAGCTTGATTGACATAC
      S  A  E  L  A  R  Y  P  K  L  K  S  M  L  I  E  V  I  S  E  L  L  R  E  R  L  Q  P  T  R  S  Y  V  E  S  L  I  D  I  H  525

2041 ATCGAGCCTACATCAATACTAATCATCCTAATTTTTTAAGTGCAACAGAAGCAATGGATGACATCATGAAAACGCGTAGAAAACGGAATCAAGAGTTATTGAAAAGTAAGTTGTCTCAAC
      R  A  Y  I  N  T  N  H  P  N  F  L  S  A  T  E  A  M  D  D  I  M  K  T  R  R  K  R  N  Q  E  L  L  K  S  K  L  S  Q  Q  565

2161 AGGAGAATGGACAAACCAACGGTATTAATGGTACTTCATCTATCTCTTCGAATATAGATCAAGATTCTGCTAAAAACAGTGACTACGATGATGATGGTATCGACGCAGAATCGAAGCAAA
      E  N  G  Q  T  N  G  I  N  G  T  S  S  I  S  S  N  I  D  Q  D  S  A  K  N  S  D  Y  D  D  D  G  I  D  A  E  S  K  Q  T  605

2281 CGAAGGACAAATTTTTAAATTATTTCTTTGGCAAGGATAAAAAGGGTCAACCTGTGTTCGATGCATCAGACAAGAAAAGATCCATTGCCGGTGATGGAAATATTGAAGATTTTAGAAATT
      K  D  K  F  L  N  Y  F  F  G  K  D  K  K  G  Q  P  V  F  D  A  S  D  K  K  R  S  I  A  G  D  G  N  I  E  D  F  R  N  L  645

2401 TACAAATATCAGATTTTTCACTGGGCGATATAGATGACCTTGAAAACGCTGAACCTCCACTGACCGAGAGAGAAGAATTGGAGTGCGAATTAATTAAACGTCTGATTGTTTCATACTTTG
      Q  I  S  D  F  S  L  G  D  I  D  D  L  E  N  A  E  P  P  L  T  E  R  E  E  L  E  C  E  L  I  K  R  L  I  V  S  Y  F  D  685

2521 ATATTATAAGAGAAATGATTGAAGATCAAGTACCAAAGGCAGTTATGTGTTTACTCGTCAATTATTGTAAGGATTCTGTTCAAAACAGATTGGTAACCAAACTCTACAAAGAAACACTGT
      I  I  R  E  M  I  E  D  Q  V  P  K  A  V  M  C  L  L  V  N  Y  C  K  D  S  V  Q  N  R  L  V  T  K  L  Y  K  E  T  L  F  725

2641 TTGAAGAACTTTTAGTTGAGGATCAAACTTTAGCTCAAGATAGAGAACTATGTGTGAAATCACTCGGAGTTTATAAAAAGGCTGCAACCCTTATTAGTAATATTCTGTAATTGCATAATT
      E  E  L  L  V  E  D  Q  T  L  A  Q  D  R  E  L  C  V  K  S  L  G  V  Y  K  K  A  A  T  L  I  S  N  I  L  *              761

2761 CATCTCATTTTTGATCTTACTTCAACATTGCGGGCGTGATTATAGGTCAGTGTTTATTCCTTTACTCAGTTGATGATTTCAAATGTGCTCTCCTCTCCATTCTTTTTCTTGTTAATAAAA
2881 ATCCATAACTAAATAAATAACAAATATTAGCAATCGCAAAAGTATTAACTAAGCTAGAGAACCTTCACTAGAGAAGCTCTACCTAAAGGTATAGAACAGGAAAAAGTGTTTTTATTTTGG
```

Figure 1. (*A*) Map of the insertion and deletion at the *DNM1* locus. Restriction sites shown are as follows: *H*, HindIII; *B*, BglII; *P*, PstI; *E*, EcoRI; *X*, XbaI; *M*, MluI. *CEN12* is depicted as a black dot. The numbers below the *DNM1* gene correspond to the numbers in the sequence in *B*. The numbers below the *URA3* containing fragment correspond to those published in Sikorski and Hieter (1989). (*B*) The nucleotide sequence of the *DNM1* gene. The open reading frame for Dnm1p is shown below the nucleotide sequence. The numbers in the left hand column are for the nucleotide sequence and the numbers in the right hand column are for the amino acid sequence. The arrows show the location and orientation of the degenerate primers discussed in the Materials and Methods. The CGARRI box marks the end of extensive homology between the dynamins and the Dnm1p/Vps1p sub-group. The consensus GTP binding site is indicated by asterisks. Sequence data are available from EMBL/Genbank/DDBJ under accession number L40588.

chromosome 12 was further defined using an ordered yeast genomic library. A probe from within the *DNM1* gene hybridized with clone 4355 from the prime λ phage library. A map of the phage clone suggested that *DNM1* might be linked to *CEN12*. Genetic mapping confirmed that *DNM1* is tightly linked to a fully functional centromere (data in Gammie and Rose, in press). Sequence analysis revealed that *DNM1* is the most proximal gene to the right of *CEN12* and is oriented such that transcription would proceed towards the centromere (Fig. 1 *A*). The chromosomal configuration of *DNM1* is strikingly similar to *VPS1*, another dynamin-related gene, which is immediately adjacent to *CEN11* and also is oriented with the reading frame directed toward the centromere (Yeh et al., 1991).

Nucleotide sequence analysis showed that the 2.3-kb open reading frame of the *DNM1* gene encodes a putative protein of 85 kD, designated Dnm1p (Fig. 1 *B*). Like other dynamin-related family members, Dnm1p contains a tripartite GTP binding consensus site in the amino-terminus (starred residues, Fig. 1 *B*). A dendrogram of representative family members (Fig. 2) allowed for the classification of four subgroups, each named for a prototypic member: dynamin, Vps1p, Mx, and Mgm1p. The Mgm1p subgroup at present contains a single member. Dnm1p and Vps1p are placed in a separate subfamily, although the homology of these proteins with dynamin extends quite a bit beyond that which is detected for the Mx proteins and Mgm1p. For example, Dnm1p, Vps1p, and the dynamin/shibire isoforms, but not the other superfamily members, contain a S/CGARRI box (amino acids 397–404 in Dnm1p). This site marks the carboxy-terminal end of the highly homologous region for Dnm1p and Vps1p with the dynamin/shibire subgroup.

In spite of the extended homology, Dnm1p and Vps1p lack structural elements correlated with important functional properties in the dynamins. Dynamin and shibire isoforms contain a pleckstrin homology (PH) domain (Haslam et al., 1993), corresponding to amino acids 510–633 in dynamin. The PH domain is postulated to be important for protein-protein interaction or for membrane association (Ferguson et al., 1994). The homology of Dnm1p and Vps1p with the dynamins is extremely low in the region corresponding to the PH domain, suggesting that the regulatory signals for Dnm1p and Vps1p are different. Moreover, Dnm1p and Vps1p also lack a proline-rich extension in the carboxy-terminal region, shown to be important for regulating the GTPase activity of dynamin (Herskovits et al., 1993*b*).

Proline-rich tails are present in all of the dynamin and shibire isoforms isolated thus far. Microtubules (Shpetner and Vallee, 1992), acid phospholipids (Tuma et al., 1993), and certain SH3 containing proteins (Booker et al., 1993; Gout et al., 1993; Herskovits et al., 1993b; Ando et al., 1994; Miki et al., 1994; Scaife et al., 1994; Seedorf et al., 1994) can bind to the carboxy-terminal proline-rich region and stimulate the GTPase. In addition, protein kinase C phosphorylation sites appear to reside primarily in this proline-rich extension (Liu et al., 1994). Phosphorylation by protein kinase C also stimulates the GTPase of dynamin (Robinson et al., 1993). Hence, two regions thought to be important regulatory domains in dynamin, the PH domain and the proline-rich tail, are lacking in the yeast proteins Dnm1p and Vps1p.

Dnm1p and Vps1p share other distinguishing features. In the extended superfamily the conserved GTPase domain is often interrupted by a region with low homology of variable length (from 2–46 amino acids). Dnm1p and Vps1p possess the largest spacer regions, which are of comparable size (44 and 46 amino acids respectively) and charge (estimated pI of 4.7 and 5.7, respectively). The functional significance of these spacers is unknown.

Direct sequence comparisons showed that Dnm1p is most like Vps1p. However, using a program that allowed for significant gaps, Vps1p is as related to dynamin and shibire as it is to Dnm1p with respect to total amino acid sequence identity (Fig. 2). However, both Dnm1p and Vps1p are more like shibire in the conserved amino-terminal portion of the protein than they are to each other, suggesting that what has been conserved from a common progenitor is not the same in the two yeast proteins (Fig. 2). Dnm1p and Vps1p are most like each other in the carboxy-terminal region, with the *Caenorhabditus elegans* dynamin (Dyn1) being the next closest relative in that less conserved domain. Finally, both Dnm1p and Vps1p are most distantly related to the third yeast family member,

	Dnm1p			Vps1p			Dynamin I			Dynamin II			shibire			Dyn1			Mx		
	T	N	C	T	N	C	T	N	C	T	N	C	T	N	C	T	N	C	T	N	C
Vps1p	44	52	33																		
Dynamin I	41	55	26	45	59	29															
Dynamin II	41	55	27	45	59	29	81	88	76												
shibire	42	56	27	45	60	29	68	78	61	69	80	61									
Dyn1	41	53	29	45	56	32	64	74	57	63	77	54	66	76	59						
Mx	31	39	18	31	40	21	31	40	20	32	40	21	32	39	20	31	38	20			
Mgm1p	30	37	20	29	36	22	28	35	17	28	34	22	29	34	22	26	34	18	24	30	17

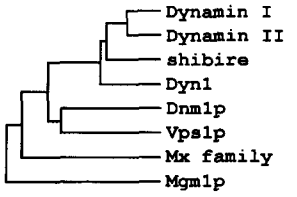

Figure 2. (*A*) The total protein (*T*), the amino-terminal (*N*), and the carboxy-terminal (*C*) regions of the proteins were compared using the Gap program of the Wisconsin Package with a gap weight of 3.0 and a gap length of 0.1. The amino-terminal region corresponded to the 350–400 amino acids that end with the S/CGARRI box described in Fig. 1 *B*, while the carboxy-terminal region was from the end of that box to the stop codon for each protein. The percent identity is shown for the various sequence pairs. The sequences were obtained from Genbank with the following accession numbers. Rat brain dynamin I (P21575); Rat dynamin II (L25605/L24562); *Drosophila melanogaster* shibire (X59435/X59448/X59449); *Caenorhabditus elegans* Dyn1 (L29031); yeast Vps1p (M33315/X54316); yeast Dnm1p (L40588); rat Mx1 (P118588); yeast Mgm1p (L07419/X62834). (*B*) Dendrogram of representative family members. The dendrogram was produced by the Pileup program of the Wisconsin Package with a gap weight of 3.0 and a gap length of 0.1. The same sequences were used as described in *A*.

Mgm1p. Taken together, the sequence comparisons suggest that Dnm1p is not the cognate homologue of dynamin.

A DNM1 Deletion Mutant Is Viable

Both a disruption of *DNM1* within the highly conserved GTPase region, and a complete deletion of the gene (Fig. 1 *A*) showed that the protein is not essential for life under a variety of growth conditions. Isogenic single, double and triple deletion strains were constructed with the three yeast dynamin-related genes, *DNM1*, *VPS1*, and *MGM1*, to determine if any of the known family members are functionally redundant. All of the mutant strains were viable indicating that the family members do not share an essential overlapping function. A nonessential, redundant function might exist, but was not detected in the vacuolar protein sorting or mitochondrial function assays that we performed.

Although viable, each of the yeast dynamin-related deletion strains had a unique profile for growth on different carbon sources. All of the strains were able to grow on glucose, even at elevated temperatures. Consistent with a strong mitochondrial defect, each strain containing a deletion at the *MGM1* locus was unable to grow on any of the non-fermentable carbon sources, regardless of the temperature.

In contrast, *dnm1* and *vps1* disruption strains showed impaired utilization for certain non-fermentable carbon sources. However, these defects were evidenced primarily at elevated temperatures, e.g., 37°C. Mutant *dnm1* strains showed impaired growth on ethanol and acetate, while *vps1* strains did not grow well on glycerol, lactate, and acetate. The effects were superimposable in that the *dnm1 vps1* double mutant was defective for use of all of the non-fermentable carbon sources tested. Ethanol and acetate are two-carbon compounds that require normal peroxisomal and mitochondrial function to be metabolized. In contrast, glycerol and lactate breakdown requires only normal mitochondrial function. Therefore, the *dnm1* defects may be due to impaired peroxisomal function.

One consequence of the impaired utilization of acetate in the *dnm1* mutant may be the observed deficiency in sporulation. As is the case with *vps1/spo15* (Yeh et al., 1991), homozygous *dnm1* diploid strains showed a sporulation defect (47% of wild type); however, the effect was not as severe as *vps1*, which was unable to sporulate. In summary, since *dnm1* and *vps1* deletion strains show only subtle temperature-sensitive growth defects on certain nonfermentable carbon sources, we concluded that these phenotypes were most likely due to indirect effects of their principal roles in the cell.

Dnm1p Is Not Involved in Sorting or Secretion of the Vacuolar Proteins CPY and Pho8p

Given the high degree of homology between Vps1p and Dnm1p we checked for defects in vacuolar protein sorting in *dnm1* disruption strains. Carboxypeptidase Y (CPY) is a soluble vacuolar protein used to identify vacuolar protein sorting mutants (reviewed in Rothman et al., 1989). In wild type, CPY is found in three forms, the two glycosylated precursors (P1) and (P2), and the mature, proteolytically cleaved form (m-CPY). m-CPY is produced from the P2 form only after successful delivery to the vacuole. The predominance of m-CPY in the cell is indicative of proper vacuolar protein sorting. If CPY is not sorted correctly, the P2 form is secreted into the culture medium.

Western blotting analysis with α-CPY antibody showed that a *dnm1* disruption strain and the isogenic wild-type control do not accumulate appreciable levels of P2 in the culture medium, whereas *vps1* deletion strains did secrete the P2 form (Fig. 3 *A*). The sorting defect of *vps1* was unaffected in the *dnm1 vps1* double mutant. The Western blot analysis of the cell pellets also showed that the *dnm1* disruption strain was indistinguishable from the isogenic wild-type control, both of which contain m-CPY, while in the *vps1* strains no m-CPY was detectable. The upper band present in all four lanes for the cell pellet fractions is a cross-reacting band with slower mobility than all of the forms of CPY (compare cell pellet lanes with lanes *3* and *4* containing the largest form, P2).

Although the *dnm1* strain did not appear to have a CPY sorting defect by Western analysis, we performed pulse–

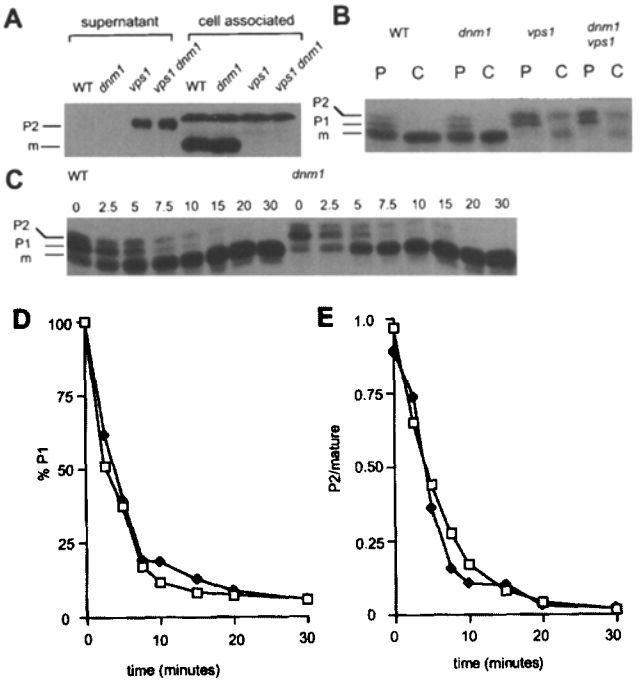

Figure 3. The sorting of the soluble vacuolar protein CPY. *A* shows a Western blot of CPY in the culture supernatants (first four lanes) and in the cell pellets (last four lanes) of strains isogenic except for the indicated disruptions (*dnm1* for *dnm1::HIS3*, *vps1* for *vps1::LEU2*). WT is for wild type, the control. The strains for these experiments are discussed in the Methods and Materials and listed in Table I. The two of the three forms of CPY (discussed in the Results) are marked to the left of the Western, since only P2 and mature forms were detected in this assay. *B* shows a pulse (*P*) of 15 min, and a chase (*C*) of 30 min of CPY in strains isogenic except for the indicated disruptions. The three forms of CPY are indicated to the left of the lanes. *C* shows a time course of processing of CPY in wild-type (*WT*) and *dnm1* strains. The cells were pulsed for 10 min, and chased for 0, 2.5, 5.0, 7.5, 10, 15, 20, and 30 min. Graphs of the normalized counts over time of the P1 form (*D*) and of the P2/mature ratio (*E*) are shown for WT (*open squares*) and *dnm1* (*black diamonds*).

chase experiments to examine the extent and rate of CPY sorting. The first experiment compared the four strains described for the Western blot. For the *dnm1* disruption strain and the isogenic wild-type control, the ratios of the forms of CPY in the pulse, and the levels of m-CPY in the chase were indistinguishable. In contrast, *vps1* strains showed strong defects in CPY processing. Again, we found that the *vps1* defect was unaffected by a disruption of the *DNM1* gene (Fig. 3 *B*).

To determine whether the rate of sorting was altered in a more subtle fashion, we performed an extensive time-course of sorting for the *dnm1* and isogenic wild-type control. Quantitative analyses of the time course of processing of CPY showed that the disappearance of P1 (Fig. 3, *C* and *D*) and the concomitant loss of P2 and accumulation of m-CPY (Fig. 3, *C* and *E*) were indistinguishable for the *dnm1* mutant and the wild-type control. We conclude from these data that Dnm1p was not required for the rate of sorting of the soluble vacuolar protein CPY.

From the CPY experiments we may also conclude that *dnm1* strains do not have an obvious secretory defect. Accumulation of P1 found in the endoplasmic reticulum, or of the Golgi-associated P2 form would have indicated a possible early secretory defect. We observed that pre-CPY forms did not accumulate in *dnm1* strains when compared to the wild-type strain. Therefore, Dnm1p is unlikely to play a role in early secretion. Strains with a disruption in the *DNM1* gene also do not appear to have a late secretory defect since the CPY levels secreted in *vps1* is the same as in the *vps1 dnm1* double mutant (Fig. 3 *A*). In addition if late secretion were affected, we would have expected to see P2-CPY accumulate in the double mutant cells during the pulse–chase, but the levels were unchanged when compared with the *vps1* single mutant (Fig. 3 *B*).

Membrane and soluble proteins have been reported to have different requirements for proper sorting to the vacuole (reviewed in Nothwehr and Stevens, 1994). For this reason we performed a pulse–chase experiment to follow the fate of a membrane associated vacuolar protein, Pho8p. The rate of loss of the Pho8p precursor and accumulation of the mature form occurred with identical kinetics in the *dnm1* and wild-type strains (Fig. 4 *A*). The half life of the precursor for both strains was ~5 min. We therefore conclude that Dnm1p is also not required for sorting of the membrane associated vacuolar protein Pho8p. These data, combined with the results from the CPY experiments, allowed us to conclude that Dnm1p does not participate in the primary cellular role of its highly homologous family member Vps1p.

dnm1 Mutant Strains Are Not Defective for Lucifer Yellow Accumulation, a Marker for Fluid Phase Endocytosis

For Dnm1p, the next most homologous subfamily of dynamin-related proteins is comprised of the dynamin/shibire isoforms. Given this homology and that dynamin/shibire isoforms are involved in endocytosis, we tested *dnm1* disruption strains for endocytic function. The accumulation of Lucifer Yellow within the vacuole is an assay for fluid-phase endocytosis (Dulic et al., 1991). The uptake of LY is time and energy dependent (Riezman 1985), and requires certain proteins important for endocytosis (Munn and Riezman, 1994 and references therein).

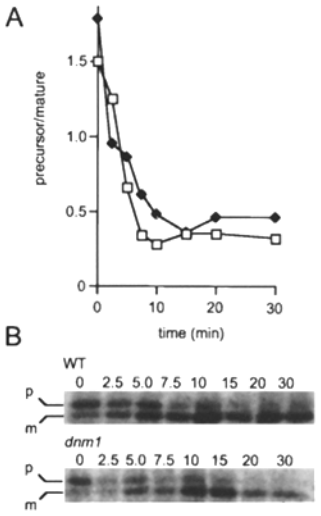

Figure 4. Pulse–chase analysis of Pho8p, a membrane-associated vacuolar protein. *A* shows a time course of processing of Pho8p in wild-type, WT, (*open squares*) and in *dnm1* (*black diamonds*) strains. The cells were pulsed for 10 min, and chased for 0, 2.5, 5.0, 7.5, 10, 15, 20, and 30 min. The plot is of the ratio of precursor to mature Pho8p over time. *B* is an image of the gel used to quantitate. The precursor (*p*) and mature (*m*) forms of Pho8p are indicated to the left.

Looking at various time points (30, 60, and 90 min), we found that the LY accumulation in *dnm1* strains (Fig. 5 *D*)

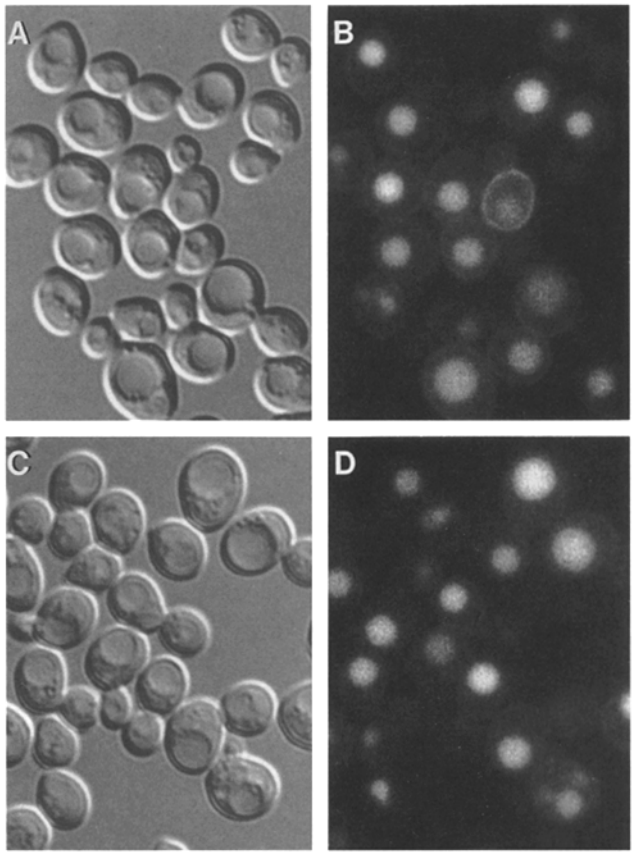

Figure 5. Lucifer yellow accumulation. Exponentially growing cells were incubated for 0.5, 1.0, and 1.5 h in the presence of LY. The 1.0-h time point is shown in the figure. After washing the cells were visualized by Nomarski optics (*A* and *C*) to assess the overall cell morphology, and in particular, to identify the vacuole (large, round organelle creating a dented appearance). FITC filter sets were used to visualize the LY (*B* and *D*). *A* and *B* are wild-type *DNM1* control cells and *C* and *D* are *dnm1* mutant cells.

was indistinguishable from the wild-type control (Fig. 5 *B*). These data indicate that there is no obvious fluid-phase defect associated with a disruption of the *DNM1* gene. However, although the extent of accumulation looked identical in the two strains, a minor effect on the rate of fluid-phase endocytosis might not be detected by these methods.

Finally, Nomarski optics showed that the vacuolar morphology of *dnm1* (Fig. 5 *C*) is identical to the isogenic wild-type control (Fig. 5 *A*), a condition that is necessary for proper assessment of LY accumulation. From the vacuolar morphology of the Nomarski and LY uptake images, we may also conclude that *dnm1* strains are not class C *vps* mutants, which lack coherent vacuoles (Raymond et al., 1992).

Disruption of the DNM1 Gene Results in a Lag in Recovery from Pheromone Arrest

Our LY data suggested that there was no obvious fluid-phase endocytic defect in the *dnm1* mutant. However, a role for Dnm1p in receptor-mediated endocytosis had not been excluded. It is of interest that dominant-negative mutations in mammalian dynamin affect receptor-mediated, but not bulk fluid-phase, endocytosis (Herskovits et al., 1993a; Damke et al., 1994).

Initial evidence for a role for Dnm1p in receptor-mediated endocytosis came from our analysis of the recovery from growth arrest after treatment with pheromone. When yeast are exposed to the appropriate mating pheromone, the cells arrest in G1 in preparation for mating (reviewed in Sprague and Thorner, 1992). If a cell fails to mate, recovery from G1 arrest ultimately occurs. The recovery response is thought to be dependent on several variables: (*a*) removal of ligand from the extracellular environment via a secreted protease; (*b*) inhibition of the intracellular signaling pathway; and (*c*) receptor down-regulation, including endocytosis (reviewed in Sprague and Thorner, 1992).

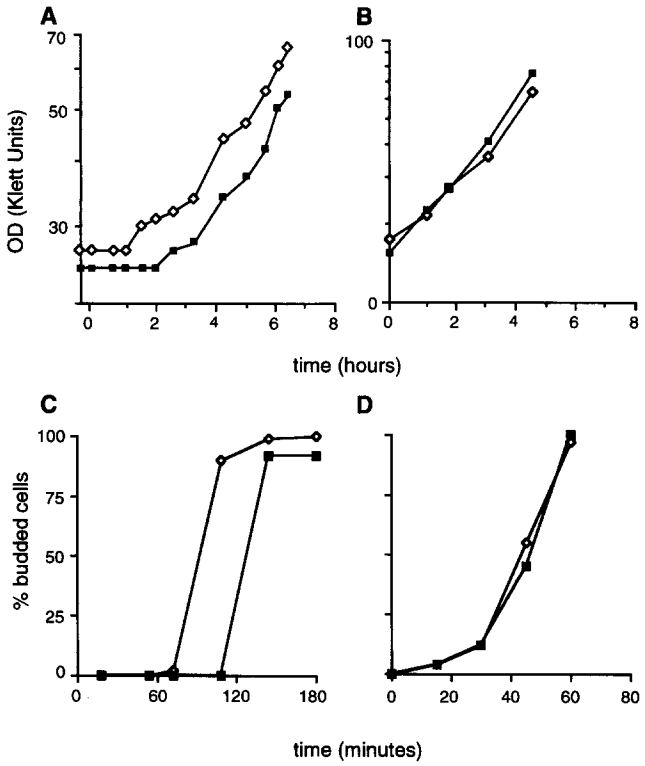

Figure 6. Delay in recovery from pheromone arrest. The figure shows the recovery of *dnm1* (*black squares*) and of the wild-type *DNM1* control (*open diamonds*) from (*A*) pheromone arrest, and (*B*) stationary phase arrest, plotted for OD (Klett Units); and from (*C*) pheromone arrest, and (*D*) *cdc28-4* G1 arrest plotted for bud emergence over time in min.

We found that the *dnm1* disrupted strain showed a defect in recovery from α-factor induced G1 arrest when compared with an isogenic wild-type control strain. The effect was first seen when *dnm1* cells failed to fill in a halo of growth arrested cells generated by α-factor spots in plate assays (data not shown). We quantitated this defect using liquid cultures. After removing pheromone from the arrested cells, we found that *dnm1* strains lagged significantly behind the control strain (Fig. 6, *A* and *C*).

The liquid assays were performed with *MAT***a** strains lacking Bar1p, a protease that degrades extracellular α-factor (reviewed in Sprague and Thorner, 1992). The delay was quantitated by several methods: culture optical density, colony forming units, and bud formation. Changes in colony forming units (not shown) and in culture optical density (Fig. 6 *A*) corresponded to when daughter cells were liberated from the mother cell. These methods showed that the delay was ~90 min. Bud formation was more sensitive for detecting when the cells resumed normal growth. The delay measured by this method was ~60 min (Fig. 6 *C*).

Two controls were performed to ensure that the defect was specific to recovery from pheromone arrest rather than cell cycle arrest. There was no difference between disrupted and control *DNM1* strains in the recovery after stationary phase arrest (Fig. 6 *B*). In addition, the *dnm1* disruption strains resumed growth after G1 arrest with wild-type kinetics. We analyzed the rate of bud formation after releasing the cells from G1 arrest caused by a temperature sensitive mutation in the *CDC28* gene. After release, there was no difference between the *dnm1* disrupted and *DNM1* control strains (Fig. 6 *D*). Hence, the *dnm1* strains showed a lag in recovery specifically from pheromone arrest, a finding that is consistent with a receptor-mediated endocytic defect.

Disruption of DNM1 Delays the Turnover of the Ste3p Pheromone Receptor

Davis et al. (1993) developed a screen to obtain mutants with receptor-mediated endocytic defects. The screen relied on the fact that *MAT*α cells must express Ste3p receptors to mate (Michaelis and Herskowitz, 1988) and that the receptors are rapidly turned over (Davis et al., 1993). An enhanced ability to mate after turning off Ste3p synthesis is the initial criterion for an endocytic defect in the screen. Quantitative matings were performed to determine whether *dnm1* disruption strains exhibited an increased ability to mate after blocking Ste3p synthesis. The data from these experiments reflect receptor function over the period of mating (6 h). The time points signify the time elapsed be-

Table II. Quantitative Mating of MATα dnm1and Wild Type After Repression of Ste3p Synthesis

Strain (MATα)	Diploids Formed			Mating Efficiency		
	0 min	15 min	60 min	0 min	15 min	60 min
					diploids/total cells*	
dnm1	2.7×10^5	2.0×10^4	9.8×10^2	1.0	0.063	0.0034
Wild type	9.7×10^4	4.7×10^3	3.7×10^2	0.32	0.014	0.0010

*Diploids assayed by complementation of auxotrophic markers after matings on glucose of *MAT***a** cells to the *MAT*α cells which received no prior repression (0 min) or repression of Ste3p synthesis with glucose for 15 or 60 min before mating.

tween receptor repression and exposure to the mating partner. These experiments showed that the *dnm1* strain mated threefold more efficiently than did the isogenic wild-type control at all time points (Table II). These data suggested that the Ste3p receptor functioned longer in the *dnm1* disruption strain than in the wild type. This effect was not as strong as that reported for a mutation affecting the late endosome, *ren1-1* (Davis et al., 1993). However, the extent of the defect is similar to that reported for a *pep4* deletion mutant, in which the receptor half-life is increased (Davis et al., 1993). In summary, the data from the quantitative matings are consistent with a defect in the pathway leading to the turnover of the Ste3p receptor.

We determined the half life of the Ste3p pheromone receptor using pulse–chase analyses. These experiments allowed us to assay more directly for an endocytic defect in *dnm1* disruption strains. Routinely, after immunoprecipitation with α-Ste3p antibody, a single major band was detectable upon autoradiography (Fig. 7 *B*). Based on independent experiments we found that the rate of Ste3p turnover decreased 2.4 ± 0.6-fold in the *dnm1* disruption strain over the isogenic wild-type control (Fig. 7 *A*), thereby changing the half life from 20 min for wild type to 40–60 min for *dnm1* mutant strains. These data suggested that Dnm1p is involved in the constitutive turnover of the Ste3p receptor. The pulse–chase experiments assay total cellular protein and do not identify the cellular localization of the receptor. Therefore, we wanted to next determine if the defect was a consequence of impaired internalization, or inefficient delivery of the receptor to the vacuole.

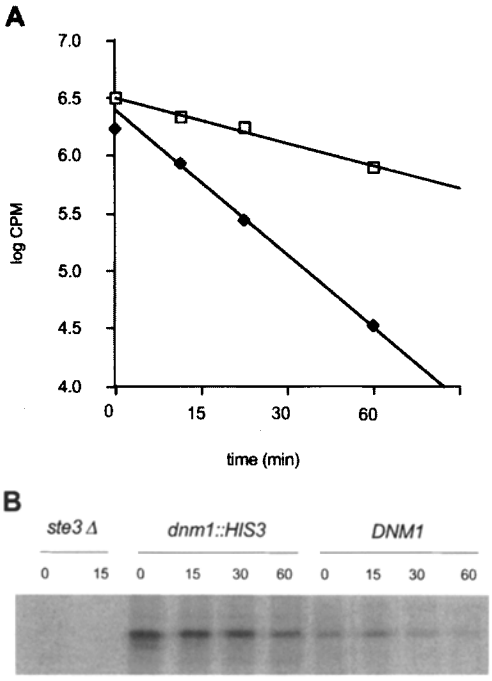

Figure 7. Pulse–chase analysis showing Ste3p turnover in *dnm1::HIS3* and in wild-type *DNM1* strains. In *A*, the graph shows the log of counts per min (*CPM*) as was obtained by PhosphorImager analysis (see Materials and Methods) over time in min after the chase. The graph is the combined data from two experiments. The gel in *B* is the image from one of the experiments. *DNM1* is the isogenic wild type strain MS3107 *DNM1*, *dnm1::HIS3* is strain MS3031, and *ste3*Δ is strain SY1372. Open squares are for *dnm1* and the black squares are for *DNM1*.

Dnm1p Does Not Act at the Earliest Step in Endocytosis of ^{35}S-α-Factor

The early steps of receptor-mediated endocytosis, binding and internalization of ligand, were examined quantitatively using ^{35}S-α-factor. The rate and extent of internalization in the *dnm1* disruption strain were indistinguishable from the isogenic control strain (Fig. 8). We observed a half time of internalization of 15 min for both strains. A two- to threefold difference in the kinetics of uptake would have given an easily detected difference in the half-time for internalization of 30–45 min for *dnm1* rather than the observed 15 min. Hence, a lag in internalization would have significantly shifted the curve to the right for *dnm1*. From these data, we conclude that the rate and extent of the earliest step of receptor-mediated endocytosis seemed to be unaffected by the *dnm1* disruption. These experiments suggested that the *dnm1* defect must be accounted for in later steps of endocytosis.

A Disruption of DNM1 Impedes Delivery of Ste3Δ365p to the Vacuole During Ligand-induced Endocytosis

The steps in the endocytic pathway that are subsequent to internalization involve transit of endosomes to the vacu-

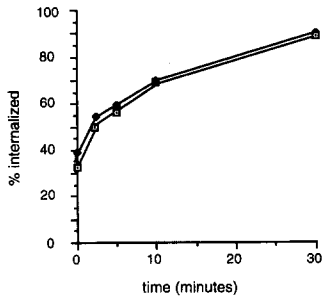

Figure 8. Uptake of ^{35}S-α-factor in *dnm1::HIS3* (*open symbols*) and in wild-type *DNM1* control strains (*black symbols*). The % internalized represents the acid resistant counts (0.05 M sodium citrate, pH 1.1 washes) over the total bound counts (0.1 M potassium phosphate, pH 5.8 washes). Binding of pheromone was at 0°C for 1 h and internalization proceeded at 30°C for the times indicated on the graph. The graph represents the average of five experiments.

ole. The fate of the Ste3p pheromone receptor after removal from the plasma membrane can be traced using immunofluorescence (Davis et al., 1993). Normally Ste3p is endocytosed by both the constitutive and ligand-induced pathways (Davis et al., 1993). A truncation of Ste3p, designated Ste3Δ365p, fails to be turned over effectively via the constitutive pathway but will be internalized upon exposure to the **a**-factor ligand (Davis *et al.*, 1993). Therefore, the Ste3Δ365p deletion construct allowed us to examine the ligand-induced endocytic pathway specifically. An epitope-tagged, Ste3Δ365p was expressed in galactose containing media via a galactose regulated promoter, and receptor synthesis was shut off by the addition of glucose to the cultures. An extract containing **a**-factor was also added, to trigger ligand-induced endocytosis and time points were taken 0.5, 1.0, and 1.5 hours after exposure. The experiments were conducted in *MATα* strains with a deletion in *PEP4*, to prevent intracellular degradation, allowing delivery of the tagged receptor to the vacuole to be assessed by immunofluorescence.

Before exposure to pheromone, the wild-type and *dnm1* strains both showed the expected surface staining (Fig. 9, *A–D*). Receptor synthesis was shut off with glucose, and the controls were exposed to extracts containing α-factor, for which *MATα* cells have no receptor. Under these control conditions, after 0.5, 1.0, and 1.5 h the cells continued to show prominent surface staining (98% of stained cells for both wild-type and *dnm1* strains) (Fig. 9, *E–H*), indicating that the receptor had been retained on the surface in the absence of true ligand. Some staining was detectable in the vacuole of both strains over time (for example, see *F*), however the predominant staining was on the surface.

In the experimental condition, further receptor synthesis was blocked with glucose and the cells were exposed to **a**-factor extracts, the true ligand. These conditions revealed a major difference between the *dnm1* and the wild-type *DNM1* control strains. Internalization and delivery to the vacuole in the *DNM1* strain proceeded rapidly, and the receptor was found predominantly in the vacuole (88% of the stained cells by 1.5 h) (Fig. 9, *I–J*). As early as 30 min after exposure to ligand, the majority of the staining was in the vacuole for the wild-type strain (data not shown). Staining of the vacuole with a vacuolar specific antibody confirmed that the large organelle visualized with Nomarski optics is indeed the vacuole (data not shown). In addition, under identical conditions, except that Pep4p was functional, the staining with the α-c-myc antibody disappeared rapidly (within 30 min) after **a**-factor exposure for the wild-type *DNM1* strain, showing that the receptor was being efficiently delivered to the vacuole, the organelle containing Pep4p-dependent degradative activity (data not shown).

After exposure to **a**-factor pheromone, the staining pattern in the *dnm1* disruption strain differed significantly from the wild-type control strains. For both strains, the majority of the Ste3Δ365p receptor was cleared from the surface within 30 min after ligand addition (data not shown). In the wild type, vacuolar staining was seen within 30 min to 1 h. However, in 90% of the *dnm1*-stained cells, the protein was not delivered to the vacuole even after 1.5 h (Fig. 9, *K–L*). Vacuolar-exclusion was observed to a limited extent in wild type at the earliest time point (30 min, data not shown), suggesting that the *dnm1* phenotype is a lag in the normal pathway, and not a condition peculiar to the mutant.

The staining pattern in *dnm1* is different from that exhibited by another endocytosis mutant, *ren1*, where the receptor is concentrated in a pre-vacuolar compartment, or endosome (Davis et al., 1993). In addition, the localization of Ste3Δ365p within the *dnm1* cells was not affected in a

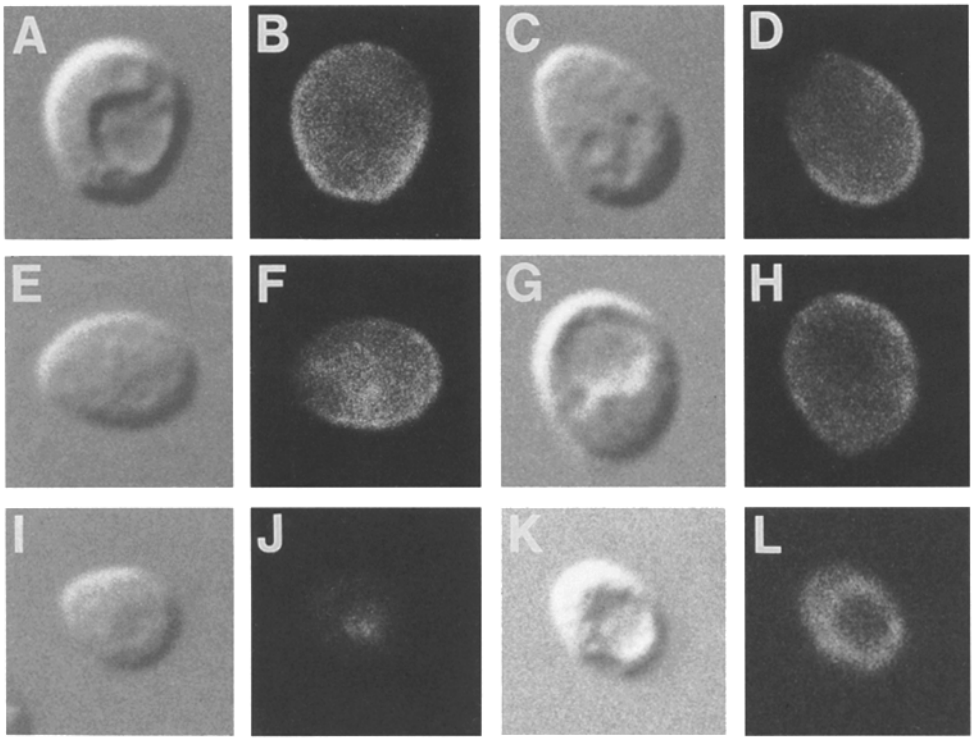

Figure 9. Immunofluorescence of Ste3Δ365p after exposure of pheromone. *A, C, E, G, I,* and *K* are the Nomarski images of the cells and *B, D, F, H, J,* and *L* are the corresponding FITC image of the cells showing Ste3Δ365p localization before pheromone treatment (*B* for wild-type *DNM1* and *D* for *dnm1*), 1.5 h after mock pheromone treatment (*F* for wild-type *DNM1* and *H* for *dnm1*), and 1.5 h after **a**-factor treatment (*J* for wild-type *DNM1* and *L* for *dnm1*).

PEP4 strain, indicating that the dispersed endosome-like structures did not have Pep4p-dependent hydrolytic activity (not shown). Thus, we conclude from these experiments that the *dnm1* mutant is able to internalize the receptor, but is defective for delivery of the receptor to the vacuole during ligand-induced endocytosis.

Discussion

Dnm1p and Dynamin-related Proteins

We have found that Dnm1p, a dynamin-related protein, is important in the yeast receptor-mediated endocytic pathway. In *dnm1* disruption strains, initial binding and internalization of ligand and receptor occur at normal rates, but subsequent delivery of the receptor to the vacuole is hindered. Hence, like dynamin and shibire, Dnm1p plays a role in endocytosis. However, the phenotypes of the *dnm1* disruption suggest that Dnm1p acts at a different step than the one postulated for mammalian dynamin. Unlike Dnm1p, dynamin acts at the level of internalization (van der Bliek et al., 1993; Herskovits et al., 1993*a*; Damke et al., 1994; Takei et al., 1995; Hinshaw and Schmid, 1995). Dynamin is thought to act at the level of coated vesicle formation at the plasma membrane (Hinshaw and Schmid, 1995; Takei et al., 1995). At least two explanations could account for the differences in phenotypes between dynamin and *dnm1* mutants. The disruption of the *DNM1* gene used in this study was a null mutation, while the dynamin proteins used in the endocytosis assays were dominant negatives. The dominant dynamin proteins might perturb endocytosis at an earlier stage of the process than would the absence of wild-type protein.

A more likely alternative is that Dnm1p might not be a cognate homologue of dynamin, implying that different dynamin-related proteins act at a variety of steps in the endocytic pathway. Important regulatory domains found in dynamin are lacking in Dnm1p, leading one to conclude that Dnm1p responds to different cellular cues. This conclusion leaves open the possibility that a true functional dynamin homologue exists in yeast. The degenerate primers that amplified the three known yeast family members were used in a PCR reaction with genomic DNA from a triple deletion strain. No new bands appeared, suggesting that all of the dynamin-related proteins in yeast that are detectable with these primers had been identified. However, in light of mounting sequence data from a variety of dynamin-related proteins, new primers might yield different results. Furthermore, the rapid progress of the yeast genome project will eventually reveal all of the dynamin-related family members.

The Role of Carbon Source Utilization and Endocytosis

Like other yeast genes involved in endocytosis (Raths et al., 1993), *DNM1* is not an essential gene. A disruption in *DNM1* does result in subtle growth defects at elevated temperatures on certain nonfermentable carbon sources. The metabolic deficiencies could simply reflect a generalized cellular defect such as impaired membrane functioning caused by endocytic abnormalities. For example, peroxisomal function, might be particularly sensitive to the changes caused by a *dnm1* disruption (see Results). An alternative explanation is that the role in metabolism is more direct, but not essential. One possibility is that Dnm1p-dependent endocytic function is important in a process such as autophagy. Autophagy is characterized, in part, by the rapid turnover of cytosolic glycolytic components under nutrient deficient conditions such as growth on non-fermentable carbon sources (Chiang and Schekman, 1991; Takeshige et al., 1992). At least one endocytosis mutant has been implicated in autophagy (Chiang and Schekman, 1994). Support for this hypothesis would come from direct measurements of the autophagic response in *dnm1* disruption strains.

Dnm1p and Receptor-mediated Endocytosis

Our results suggest that Dnm1p is unlikely to play a role in fluid-phase endocytosis, but is involved in both constitutive and ligand-induced receptor-mediated endocytosis. The half life of turnover during constitutive endocytosis was increased two to three fold, from 20 min for wild type to 40–60 min in a *dnm1* disruption strain. However, the block visualized during ligand-induced endocytosis showed that the majority of the receptor persisted in the cytoplasm up to 90 min. The more dramatic difference seen with the immunofluorescence assay might result from saturation of the endocytosis system with overexpressed receptor protein. Alternatively, the Ste3Δ365p receptor used in the ligand-induced assay might transit through the endocytic pathway more slowly than the full-length receptor. A final possibility is that Dnm1p may be more important for ligand-induced than for constitutive endocytosis.

Dnm1p and the Yeast Endocytic Pathway

Dnm1p seems to have a unique placement in the yeast endocytic apparatus. As discussed in the introduction, the yeast endocytic components either contribute to internalization, or affect efficient delivery of endosomes to the vacuole. In addition, all of the previously identified endocytic mutants that alter endosomal trafficking to the vacuole have either a secretory defect, or vacuolar protein sorting abnormalities. The *dnm1* mutant is unique in that the intracellular trafficking defect appears to be specific to endocytosis. The kinetics of sorting of vacuolar proteins was not affected by the *dnm1* mutation. From these results we conclude that Dnm1p is not required for vacuolar protein sorting and that the two- to threefold effect on constitutive endocytosis is not likely to be a consequence of generalized slowing of membrane trafficking events.

Previous studies have shown that internalized α-factor is found in two biochemically distinct compartments in the cell, representing early and late endosomes (Singer and Riezman, 1990; Singer-Krüger et al., 1993). In keeping with this model, Dnm1p might act before the late endosome, where the endocytic pathway merges with the post-Golgi secretory branch destined for the vacuole. This placement is consistent with the absence of a vacuolar protein sorting defect in *dnm1* mutants. An alternative explanation is that Dnm1p acts in a parallel endocytic pathway that does not merge with the late endosome used in vacuolar protein sorting.

Since Dnm1p acts at the level of delivery to the vacuole in the endocytic pathway, we must reconcile this with the

delay in recovery from pheromone arrest, and the prolonged mating in Ste3p shut-off experiments seen in the *dnm1* mutant strains. Several explanations are possible, one is that a block in delivery to the vacuole might result in a generalized slowing of the endocytic process, leaving sufficient quantities of signaling receptors on the surface to produce the in vivo effects. Surface staining of the nontruncated, fully functional **a**-factor pheromone receptor even under overexpression conditions was difficult to detect by immunofluorescence (Gammie and Rose, unpublished observations). For this reason, the possibility that some receptors are retained on the surface cannot be ruled out. However, the internalization experiments make the explanation of slowed receptor removal from the surface much less likely.

Alternatively, the intracellular block in the pathway might allow for recycling of the receptor to the surface, an effect that is not seen under normal conditions (Jenness and Spatrick, 1986). Recycling has been postulated for the phenotype of *ren1-1*, a mutation that results in defects in the late endosome (Davis et al., 1993). Our experiments suggest that if recycling is the mechanism for prolonged mating in *ren1-1* strains after repressing Ste3p synthesis, then by comparison, *dnm1* strains appear to have less efficient recycling (see the quantitative matings of Davis et al., 1993). If this hypothesis is correct, then different compartments within the cell may be more amenable to recycling. For example, recycling may be more efficient from the late endosome than from an early endosome.

A final alternative is that removal of the pheromone and receptor from the surface is not sufficient to block intracellular signaling. Endocytosis is typically thought to downregulate intracellular signaling by first causing dissociation of the ligand from the receptor and ultimately by targeting the internalized material to a degradative organelle. Binding studies (Dulic et al., 1991) have shown that α-factor binding persists in low pH (a pH of 1.1 is used to strip the ligand from the receptor). Thus, the acidity of the early endosome might be insufficient to dissociate the ligand from the receptor. In addition, the early endosome would not contain proteases in transit from the Golgi to the vacuole. Hence, in the *dnm1* disrupted strain, during delayed transit to the vacuole a pheromone–receptor complex might remain competent for transmitting the signal for the mating response. If this hypothesis is correct, our data suggest that delivery to the vacuole and subsequent degradation of the ligand–receptor complex is an important aspect of attenuation of signal transduction during the mating response.

In conclusion, one of the broader implications of our findings with Dnm1p is that the superfamily of dynamin-related proteins can act at multiple steps of vesicular trafficking. It will be of considerable interest to identify specific roles of dynamin-related proteins in other organisms in which the pathways are well characterized.

We are extremely grateful to J. Broach, T. Stevens, W. Fangman, G. Sprague, N. Davis, D. Jenness, S. Michaelis, R. Schekman, and their laboratory members for sharing antibodies, strains, and protocols used in this study. We would also like to thank members of the Rose laboratory for helpful discussions and critical reading of this manuscript.

A. E. Gammie is a post-doctoral fellow supported by a Jane Coffin Childs Memorial Fund for Medical Research. This work was also supported by a National Institutes for Health grant (GM37739) awarded to M. D. Rose.

Received for publication 30 January and in revised form 26 May 1995.

References

Ando, A., K. Yonezawa, I. Gout, T. Nakata, H. Ueda, K. Hara, Y. Kitamura, Y. Noda, T. Takenawa, and N. Hirokawa. 1994. A complex of GRB2-dynamin binds to tyrosine-phosphorylated insulin receptor substrate-1 after insulin treatment. *EMBO J.* 13:3033–3038.

Arnheiter, H., and E. Meier. 1990. Mx proteins: antiviral proteins by chance or necessity? *New Biologist.* 2:851–857.

Bénédetti, H., S. Raths, F. Crausaz, and H. Riezman. 1994. The *END3* gene encodes a protein that is required for the internalization step of endocytosis and for actin cytoskeleton organization in yeast. *Mol. Biol. Cell.* 5:1023–1037.

Booker, G. W., I. Gout, A. K. Dowing, P. C. Driscoll, J. Boyd, M. D. Waterfield, and I. D. Campbell. 1993. Solution structure and ligand-binding site of the SH3 domain of the p85α subunit of phosphatidylinositol 3-kinase. *Cell.* 75:813–822.

Chiang, H.-L., and R. Schekman. 1991. Regulated import and degradation of a cytosolic protein in the yeast vacuole. *Nature (Lond.).* 350:313–318.

Chiang, H.-L., and R. Schekman. 1994. Reply. *Nature (Lond.).* 369:284.

Chen, M. S., R. A. Obar, C. C. Schroeder, T. W. Austin, C. A. Poodry, S. C. Wadsworth, and R. B. Vallee. 1991. Multiple forms of dynamin are encoded by *shibire*, a *Drosophila* gene involved in endocytosis. *Nature (Lond.).* 351: 583–586.

Chen, M. S., C. C. Burgess, R. B. Vallee, and S. C. Wadsworth. 1992. Developmental stage- and tissue-specific expression of *shibire*, a *Drosophila* gene involved in endocytosis. *J. Cell Sci.* 103:619–628.

Chvatchko, Y., I. Howald, and H. Riezman. 1986. Two yeast mutants defective in endocytosis are defective in pheromone response. *Cell.* 46:355–364.

Cook, T. A., R. Urrutia, and M. A. McNiven. 1994. Identification of dynamin 2, an isoform ubiquitously expressed in rat tissues. *Proc. Natl. Acad. Sci. USA.* 91:644–648.

Damke, H., T. Baba, D. E. Warnock, and S. L. Schmid. 1994. Induction of mutant dynamin specifically blocks endocytic coated vesicle formation. *J. Cell Biol.* 127:915–934.

Davis, N. G., J. L. Horecka, and G. F. Sprague. 1993. *Cis*- and *trans*-acting functions required for endocytosis of the yeast pheromone receptors. *J. Cell Biol.* 122:53–65.

Dulic, V., and H. Riezman. 1989. Characterization of the *END1* gene required for vacuole biogenesis and gluconeogenic growth of budding yeast. *EMBO J.* 8:1349–1359.

Dulic, V., M. Egerton, I. Elguindi, S. Raths, B. Singer, and H. Riezman. 1991. Yeast endocytosis assays. *Methods Enzymol.* 194:602–608.

Faire, K., F. Trent, J. M. Tepper, and E. M. Bonder. 1992. Analysis of dynamin isoforms in mammalian brain: dynamin-1 expression is spatially and temporally regulated during postnatal development. *Proc. Natl. Acad. Sci. USA.* 91:644–648.

Ferguson, K. M., M. A. Lemmon, J. Schlessinger, and P. B. Sigler. 1994. Crystal structure at 2.2 Å resolution of the pleckstrin homology domain from human dynamin. *Cell.* 79:199–209.

Gout, I., R. Dhand, I. D. Hiles, M. J. Fry, G. Panayotou, P. Das, O. Truong, N. F. Totty, J. Hsuan, G. W. Booker, I. D. Campbell, and M. D. Waterfield. 1993. The GTPase dynamin binds to and is activated by a subset of SH3 domains. *Cell.* 75:25–36.

Guan, K., L. Farh, T. K. Marshall, and R. J. Deschenes. 1993. Normal mitochondrial structure and genome maintenance in yeast requires the dynamin-like product of the *MGM1* gene. *Curr. Genet.* 24:141–148.

Haslam, R. J., H. B. Koide, and B. A. Hemmings. 1993. Pleckstrin homology domain. *Nature (Lond.).* 363:309–310.

Herskovits, J. S., C. C. Burgess, R. A. Obar, and R. B. Vallee. 1993*a*. Effects of mutant rat dynamin on endocytosis. *J. Cell Biol.* 122:565–578.

Herskovits, J. S., H. S. Shpetner, C. C. Burgess, and R. B. Vallee. 1993*b*. Microtubules and Src homology 3 domains stimulate the dynamin GTPase via its C-terminal domain. *Proc. Natl. Acad. Sci. USA.* 90:11468–11472.

Hinshaw, J. E., and S. L. Schmid. 1995. Dynamin self-assembles into rings suggesting a mechanism for coated vesicle budding. *Nature (Lond.).* 374:190–192.

Ito, H., Y. Fududa, K. Murata, and A. Kimura. 1983. Transformation of intact yeast cells treated with alkali cations. *J. Bacteriol.* 153:163–168.

Jenness, D. D., and P. Spatrick. 1986. Down regulation of the α-factor pheromone receptor in *S. cerevisiae*. *Cell.* 46:345–353.

Jones, B. A., and W. L. Fangman. 1992. Mitochondrial DNA maintenance in yeast requires a protein containing a region related to the GTP-binding domain of dynamin. *Genes & Dev.* 6:380–389.

Jones, E. W. 1977. Proteinase mutants of *Saccharomyces cerevisiae*. *Genetics.* 85:23–33.

Kean, L. S., R. S. Fuller, and J. W. Nichols. 1993. Retrograde lipid traffic in yeast: identification of two distinct pathways for internalization of fluorescent-labeled phosphatidylcholine from the plasma membrane. *J. Cell Biol.* 123:1403–1419.

Kessell, I., B. D. Holst, and T. F. Roth. 1989. Membranous intermediates in endocytosis are labile, as shown in a temperature-sensitive mutant. *Proc. Natl. Acad. Sci. USA.* 86:4968–4972.

Koenig, J. H., S. Kogaku, and K. Ikeda. 1983. Reversible control of synaptic transmission in a single gene mutant of *Drosophila melanogaster. J. Neurobiol.* 14:207–225.

Kosaka, T., and K. Ikeda. 1983*a*. Possible temperature-dependent blockage of synaptic vesicle recycling induced by a single gene mutation in *Drosophila. J. Neurobiol.* 14:207–225.

Kosaka, T., and K. Ikeda. 1983*b*. Reversible blockage of membrane retrieval and endocytosis in the garland cell of the temperature-sensitive mutant of *Drosophila melanogaster, shibire^{ts1}. J. Cell Biol.* 97:499–507.

Kübler, E., and H. Riezman. 1993. Actin and fimbrin are required for the internalization step of endocytosis in yeast. *EMBO J.* 12:2855–2862.

Liu, J.-P., K. A. Powell, T. C. Südhof, and P. J. Robinson. 1994. Dynamin I is a Ca^{2+}-sensitive phospholipid-binding protein with very high affinity for protein kinase C. *J. Biol. Chem.* 269:21043–21050.

Masur, S. K., Y.-T. Kim, and C.-F. Wu. 1990. Reversible inhibition of endocytosis in cultured neurons from the *Drosophila* temperature-sensitive mutant *shibire^{ts1}. J. Neurogenet.* 6:191–206.

Michaelis, S., and I. Herskowitz. 1988. The **a**-Factor pheromone of *Saccharomyces cerevisiae* is essential for mating. *Mol. Cell Biol.* 8:1309–1318.

Miki, H., K. Miura, K. Matuoka, T. Nakata, N. Hirokawa, S. Orita, K. Kaibuchi, Y. Takai, and T. Takenawa. 1994. Association of Ash/Grb-2 with dynamin through the Src Homology 3 domain. *J. Biol. Chem.* 269:5489–5492.

Munn, A. L., and H. Riezman. 1994. Endocytosis is required for the growth of vacuolar H^+-ATPase-defective yeast: identification of six new *END* genes. *J. Cell Biol.* 127:373–386.

Nakata, T., R. Takemura, and N. Hirokawa. 1993. A novel member of the dynamin family of GTP-binding proteins is expressed specifically in the testis. *J. Cell. Sci.* 105:1–5.

Nakayama, M., K. Nagata, A. Kato, and A. Ishihama. 1991. Interferon-inducible mouse Mx1 protein that confers resistance to influenza virus is a GTPase. *J. Biol. Chem.* 266:21404–21408.

Nothwehr, S. F., and T. H. Stevens. 1994. Sorting of membrane proteins in the yeast secretory pathway. *J. Biol. Chem.* 269:10185–10188.

Nothwehr, S. F., E. Conibear, and T. H. Stevens. 1995. Golgi and vacuolar membrane proteins reach the vacuole in *vps1* mutant yeast cells via the plasma membrane. *J. Cell Biol.* 129:35–46.

Obar, R., C. A. Collins, J. A. Hammarback, H. S. Shpetner, and R. B. Vallee. 1990. Molecular cloning of the microtubule-associated mechanochemical enzyme dynamin reveals homology with a new family of GTP-binding proteins. *Nature (Lond.).* 347:256–261.

Ohashi, A., J. Gibson, I. Gregor, and G. Schatz. 1982. Import of proteins into mitochondria. *J. Biol. Chem.* 257:13042–13047.

Ozkaynak, E., and S. D. Putney. 1987. A unidirectional deletion technique for generation of clones for sequencing. *Biotechniques.* 5:770–773.

Payne, G. S., D. Baker, E. van Tuinen, and R. Schekman. 1988. Protein transport to the vacuole and receptor-mediated endocytosis by clathrin heavy chain-deficient yeast. *J. Cell Biol.* 106:1453–1461.

Poodry, C. A., and L. Edgar. 1979. Reversible alterations in the neuromuscular junctions of *Drosophila melanogaster* bearing a temperature-sensitive mutation, *shibire. J. Cell Biol.* 81:520–527.

Poodry, C. A., L. Hall, and D. T. Suzuki. 1973. Developmental properties of *shibire^{ts-1}*: a pleiotropic mutation affecting larval and adult locomotion and development. *Dev. Biol.* 32:373–386.

Raths, S., J. Rohrer, F. Crausaz, and H. Riezman. 1993. *end3* and *end4*: two mutants defective in receptor-mediated and fluid-phase endocytosis in *Saccharomyces cerevisiae. J. Cell Biol.* 120:55–65.

Raymond, C. K., I. Howald-Stevenson, C. A. Vater, and T. H. Stevens. 1992. Morphological classification of the yeast vacuolar protein sorting mutants: evidence for a prevacuolar compartment in class E *vps* mutants. *Mol. Biol. Cell.* 3:1389–1402.

Riezman, H. 1985. Endocytosis in yeast: several of the yeast secretory mutants are defective in endocytosis. *Cell.* 40:1001–1009.

Roberts, C. J., C. K. Raymond, C. T. Yamashiro, and T. Stevens. 1991. Methods for studying the yeast vacuole. *Methods Enzymol.* 194:644–661.

Robinson, P. J., J.-M. Sontag, J.-P. Liu, E. M. Fykse, C. Slaughter, H. McMahon, and T. C. Südhof. 1993. Dynamin GTPase regulated by protein kinase C phosphorylation in nerve terminals. *Nature (Lond.).* 365:163–166.

Rose, M., P. Novick, J. H. Thomas, D. Botstein, and G. R. Fink. 1987. A *Saccharomyces cerevisiae* genomic plasmid bank based on a centromere-containing shuttle vector. *Gene (Amst.).* 60:237–247.

Rose, M. D., F. Winston, and P. Hieter. 1990. Methods in yeast genetics: a laboratory course manual. Cold Spring Harbor Laboratory Press, Cold Spring Harbor, NY.

Rothman, J. H., C. T. Yamashiro, P. M. Kane, and T. H. Stevens. 1989. Protein targeting to the yeast vacuole. *Trends Biochem. Sci.* 14:347–350.

Rothman, J. H., C. K. Raymond, T. Gilbert, P. J. O'hara, and T. H. Stevens. 1990. A putative GTP binding protein homologous to interferon-inducible Mx proteins performs an essential function in yeast protein sorting. *Cell.* 61: 1063–1074.

Rothstein, R. 1991. Targeting, disruption, replacement, and allele rescue: integrative DNA transformation in yeast. *Methods Enzymol.* 194:281–301.

Sambrook, J., E. F. Fritsch, and T. Maniatis. 1989. Molecular Cloning: A Laboratory Course Manual 2nd edition. Cold Spring Harbor Laboratory Press, Cold Spring Harbor, NY.

Scaife, R., I. Gout, M. D. Waterfield, and R. L. Margolis. 1994. Growth factor-induced binding of dynamin to signal transduction proteins involves sorting to distinct and separate proline-rich dynamin sequences. *EMBO J.* 13:2574–2582.

Schandel, K. A., and D. D. Jenness. 1994. Direct evidence for ligand-induced internalization of the yeast α-factor pheromone receptor. *Mol. Cell Biol.* 14: 7245–7255.

Schimmöller, F., and H. Riezman. 1993. Involvement of Ypt7p, a small GTPase, in traffic from late endosome to the vacuole in yeast. *J. Cell Sci.* 106:823–830.

Scidmore, M. A., H. H. Okamura, and M. D. Rose. 1993. Genetic interactions between *KAR2* and *SEC63*, encoding eukaryotic homologues of DnaK and DnaJ in the endoplasmic reticulum. *Mol. Biol. Cell.* 4:1145–1159.

Seedorf, K., G. Kostka, R. Lammers, P. Bashkin, R. Daly, C. C. Burgess, A. M. van der Bliek, J. Schlessinger, and A. Ullrich. 1994. Dynamin binds to SH3 domains of phospholipase Cγ and GRB-2. *J. Biol. Chem.* 269:16009–16014.

Shpetner, H. S., and R. B. Vallee. 1992. Dynamin is a GTPase stimulated to high levels of activity by microtubules. *Nature (Lond.).* 355:733–735.

Sikorski, R. S., and P. Hieter. 1989. A system of shuttle vectors and yeast host strains designed for efficient manipulation of DNA in *Saccharomyces cerevisiae. Genetics.* 122:19–27.

Singer, B., and H. Riezman. 1990. Detection of an intermediate compartment involved in transport of α-factor from the plasma membrane to the vacuole in yeast. *J. Cell Biol.* 110:1911–1922.

Singer-Krüger, B., R. Frank, F. Crausaz, and H. Riezman. 1993. Partial purification and characterization of early and late endosomes from yeast: identification of four novel proteins. *J. Biol. Chem.* 268:14376–14386.

Singer-Krüger, B., H. Stenmark, A. Düsterhöft, P. Philippsen, J.-S. Yoo, D. Gallwitz, and M. Zerial. 1994. Role of three Rab5-like GTPases, Ypt51p, Ypt52p, Ypt53p, in the endocytic and vacuolar protein sorting pathways of yeast. *J. Cell Biol.* 125:283–298.

Sontag, J.-M., E. M. Fykse, Y. Ushkaryov, J.-P. Liu, P. J. Robinson, and T. C. Südhof. 1994. Differential expression and regulation of multiple dynamins. *J. Biol. Chem.* 269:4547–4554.

Sprague, G. F. 1991. Assay of the yeast mating reaction. *Methods Enzymol.* 194: 77–93.

Sprague, G. F., and J. Thorner. 1992. Pheromone response and signal transduction during the mating process of *Saccharomyces cerevisiae. In* The Molecular and Cellular Biology of the Yeast *Saccharomyces*: Gene Expression. Vol. II. Cold Spring Harbor Laboratory Press, Cold Spring Harbor, NY. 657–744.

Staeheli, P., O. Haller, W. Boll, J. Lindenmann, and C. Weissmann. 1986. Mx protein: constitutive expression in 3T3 cells transformed with cloned Mx cDNA confers selective resistance to influenza virus. *Cell.* 44:147–158.

Takei, K., P. S. McPherson, S. L. Schmid, and P. DeCamilli. 1995. Tubular membrane invaginations coated by dynamin rings are induced by GTP-γS in nerve terminals. *Nature (Lond.).* 374:186–190.

Takeshige, K., M. Baba, S. Tsuboi, T. Noda, and Y. Ohsumi. 1992. Autophagy in yeast demonstrated with proteinase-deficient mutants and conditions for its induction. *J. Cell Biol.* 119:301–311.

Tan, P. K., N. G. Davis, G. F. Sprague, and G. S. Payne. 1993. Clathrin facilitates the internalization of seven transmembrane segment receptors for mating pheromones in yeast. *J. Cell Biol.* 123:1707–1716.

Tuma, P. L., M. C. Stachniak, and C. A. Collins. 1993. Activation of dynamin GTPase by acidic phospholipids and endogenous rat brain vesicles. *J. Biol. Chem.* 268:17240–17246.

Vallee, R., and P. Okamoto. 1995. The regulation of endocytosis: identifying dynamin's binding partners. *Trends Cell Biol.* In press.

van der Bliek, A. M., and E. M. Meyerowitz. 1991. Dynamin-like protein encoded by the *Drosophila shibire* gene associated with vesicular traffic. *Nature (Lond.)* 351:411–414.

van der Bliek, A. M., T. E. Relelmeier, H. Damke, E. J. Tisdale, E. M. Meyerowits, and S. L. Schmid. 1993. Mutations in human dynamin block an intermediate stage in coated vesicle formation. *J. Cell Biol.* 122:553–563.

Vater, C. A., C. K. Raymond, K. Ekena, I. Howald-Stevenson, and T. Stevens. 1992. The *VPS1* protein, a homolog of dynamin required for vacuolar protein sorting in *Saccharomyces cerevisiae,* is a GTPase with two functionally distinct domains. *J. Cell Biol.* 119:773–786.

Wichmann, H., L. Hengst, and D. Gallwitz. 1992. Endocytosis in yeast: Evidence for the involvement of a small GTP-binding protein (Ypt7p). 1992. *Cell.* 71:1131–1142.

Wilsbach, K., and G. S. Payne. 1993. Vps1p, a member of the dynamin GTPase family, is necessary for Golgi membrane protein retention in *Saccharomyces cerevisiae. EMBO J.* 12:3049–3059.

Yeh, E., R. Driscoll, M. Coltrera, A. Olins, and K. Bloom. 1991. A dynamin-like protein encoded by the yeast sporulation gene SPO15. *Nature (Lond.).* 349:713–715.